Overview: State-of-the Art Commercial Membranes for Anion Exchange Membrane Water Electrolysis

Dirk Henkensmeier[1]
Center for Hydrogen and Fuel Cell Research,
Korea Institute of Science and Technology,
Seongbuk-gu, Seoul 02792, South Korea;
Division of Energy & Environment Technology,
KIST School,
University of Science and Technology,
Seoul 02792, South Korea;
Green School,
Korea University,
Seongbukgu, Seoul 02841, South Korea
e-mail: henkensmeier@kist.re.kr

Malikah Najibah
Center for Hydrogen and Fuel Cell Research,
Korea Institute of Science and Technology,
Seongbuk-gu, Seoul 02792, South Korea;
Division of Energy & Environment Technology,
KIST School,
University of Science and Technology,
Seoul 02792, South Korea
e-mail: malikahnajibah@kist.re.kr

Corinna Harms
DLR Institute of Networked Energy Systems,
Carl-von-Ossietzky-Street 15,
26129 Oldenburg, Germany
e-mail: Corinna.Harms@dlr.de

Jan Žitka
Institute of Macromolecular Chemistry,
Academy of Sciences of the Czech Republic,
162 06 Praha 6, Czech Republic
e-mail: zitka@imc.cas.cz

Jaromír Hnát
Department of Inorganic Technology,
University of Chemistry and Technology,
Prague, Technická 5,
166 28 Praha 6, Czech Republic
e-mail: Jaromir.Hnat@vscht.cz

Karel Bouzek
Department of Inorganic Technology,
University of Chemistry and Technology,
Prague, Technická 5,
166 28 Praha 6, Czech Republic
e-mail: Karel.Bouzek@vscht.cz

One promising way to store and distribute large amounts of renewable energy is water electrolysis, coupled with transport of hydrogen in the gas grid and storage in tanks and caverns. The intermittent availability of renewal energy makes it difficult to integrate it with established alkaline water electrolysis technology. Proton exchange membrane (PEM) water electrolysis (PEMEC) is promising, but limited by the necessity to use expensive platinum and iridium catalysts. The expected solution is anion exchange membrane (AEM) water electrolysis, which combines the use of cheap and abundant catalyst materials with the advantages of PEM water electrolysis, namely, a low foot print, large operational capacity, and fast response to changing operating conditions. The key component for AEM water electrolysis is a cheap, stable, gas tight and highly hydroxide conductive polymeric AEM. Here, we present target values and technical requirements for AEMs, discuss the chemical structures involved and the related degradation pathways, give an overview over the most prominent and promising commercial AEMs (Fumatech Fumasep® FAA3, Tokuyama A201, Ionomr Aemion™, Dioxide materials Sustainion®, and membranes commercialized by Orion Polymer), and review their properties and performances of water electrolyzers using these membranes. [DOI: 10.1115/1.4047963]

Keywords: AEMWE, Fumatech FAA3, Tokuyama A201, Ionomr AEMION, Dioxide Materials Sustainion, Orion Polymer Durion TM1, electrochemical separation membranes, electrolyzers

1 Introduction

This overview focuses on a selected range of membranes, which have been tested for their use in anion exchange membrane (AEM) water electrolysis, and have been or are available to researchers through companies (we refer to this as commercial membranes). We made this selection, because researchers interested in the other components of an electrolysis system (e.g., catalysts, electrodes, porous transport layers, and bipolar plates) or the system as a whole rely on membranes which are easily available and used in several labs, so that results are comparable.

1.1 Need for Anion Exchange Membrane Water Electrolysis. These days, new energy storage systems (ESS) are installed to store excess wind or solar energy. These ESS are usually based on lithium ion battery technology, because of the proven high energy efficiency, wide availability, and easy scalability, which allows to easily adjust the storage capacity. A limitation of battery-based ESS is the high cost for Li-ion batteries, which prohibits large-scale storage. However, when societies progress into renewable energy based economies, the need for multi-GW scale energy storage becomes imminent. One answer to this problem is the use of hydrogen-based ESS: Excess electric energy can be transformed into hydrogen by water electrolysis, the produced hydrogen can be stored in large tanks, underground caverns [1] or fed into the existing natural gas grid, allowing efficient transport of energy to the demand sites, where hydrogen again can be used to produce electric energy either in fuel cells or by powering gas turbines. Additional demand is foreseen for fueling fuel cell electric vehicles, which are needed to reduce the CO_2 emissions from the mobility sector, unless the charging time of batteries can be significantly reduced. In general, all needed technologies exist, and the production of hydrogen by alkaline water electrolysis is an industrial-scale process which is in operation for about 100 years.

Current alkaline water electrolysis cells are fed with 20–40 wt% KOH solution, and the electrode chambers are separated by a thick porous diaphragm (e.g., 500 μm for AGFA's Zirfon membrane [2]), which is rendered conductive by the absorbed feed solution in its pores. Problems arise when alkaline water electrolyzers are used in combination with renewable energy. They have low operational capacity (current densities between 0.2 and 0.4 A cm^{-2} are the standard) [3], are difficult to operate at large differential pressures, and have a slow response time. The low operational capacity is related to safety issues: hydrogen constantly diffuses into the oxygen

[1]Corresponding author.

Manuscript received April 10, 2020; final manuscript received July 5, 2020; published online August 24, 2020. Assoc. Editor: Kyle Grew.

stream, with which it is transported away. At very low production rates, the hydrogen concentration can reach the lower explosion limit of 4%. The upper limit is given by the high voltages, which may lead to corrosion of cell components. A technological answer to these and other disadvantages (like the large stack volume, based on the low current density) is proton exchange membrane water electrolysis (PEMWE), which was introduced in the 1960s by General Electric [4] and developed into a market-ready technology. PEMWE uses a dense proton exchange membrane and a pure water feed. It is characterized by a high efficiency, compact design, simple auxiliary systems, easy maintenance, rapid response, and a wide dynamic operation range [5–8]. However, the best performing catalysts are carbon-supported platinum on the cathode and IrO_2 on the anode side, and porous transport layers and bipolar plates are titanium based to avoid corrosion. These metals are expensive, and iridium is more scarce than platinum. Since a 100-MW PEMWE system operating at 1 A cm^{-2} requires about 150 kg iridium with an assumed catalyst loading of 2–3 mg cm^{-2}, the expected catalyst cost just for the iridium would be more than 7,000,000 US$ (48,500 US$/kg in March 2020) [9]. The large scale chosen in this calculation does not seem to be out of proportion: German ministry of economy suggested an installed electrolysis capacity target of 3–5 GW until 2030 [10].

A potential solution to this is anion exchange membrane (AEM) water electrolysis (AEMWE) [11–13]. AEMWE is a combination of alkaline water electrolysis and PEMWE: The electrode chambers are separated by a thin, dense, non-porous polymer membrane, as in PEMWE. However, charges are transferred over the membrane by hydroxide ions, as in alkaline water electrolysis, and the resulting high pH of the system reduces corrosion issues of the components: titanium in the porous transport layers (PTL) and bipolar plates (BPP) can be substituted by steel, and the scarce platinum group metals (PGM) in the electrodes can be substituted by cheap and abundant materials like nickel. In summary, AEMWE promise cheap, compact systems which can be operated at differential pressures, with a large operational capacity and fast response time.

It should be remarked that PEM water electrolysis is under constant development, and while the above-mentioned cost for the catalysts may now be about 70 US$/kW, doubling the current density, and reducing the catalyst load by 50% would reduce this to 18 US$/kW. This may be tolerable from an overall cost perspective, which targets 200–300 US$/kW for the whole system. Successful AEM technologies will need to compete with this target. If, for example, a stable AEM water electrolysis system would save 90% of the catalyst costs, but still operates at lower current density, it would be difficult to compete, unless other factors are counted in, as the potentially hazardous chemistry involved in the production of perfluorinated sulfonic acid membranes (e.g., Nafion®) and the related challenges in recycling (burning to regain the catalysts liberates HF).

1.2 Specific Challenges for Anion Exchange Membrane Water Electrolysis. Since the first journal publications on AEMWE by Wu and Scott in 2011 [14] and Leng et al. in 2012 [15], many research groups contributed to the development of AEMWE. But despite the significant progress made, e.g., increase in the current density for PGM-based systems from 0.6 A cm^{-2} [15] to 1.5 A cm^{-2} at 1.9 V [16], or even 1 A cm^{-2} in a PGM-free system [17], several challenges remain as follows:

(1) The low alkaline stability of most AEMs needs to be overcome.
(2) The ionic resistance of AEMs needs to be decreased, while retaining a low permeability for hydrogen.
(3) Many researchers still use PGM catalysts in their work because they are a convenient benchmark.
(4) The alkalinity of feed solutions should be decreased, ultimately to pure water.
(5) Suitable ionomer binders need to be developed.

Most reported systems still use alkaline feed solutions, whereas pure water is desired: (a) Water is consumed at the cathode, and the formed hydroxide ions move to the anode, where they react to water and oxygen; this leads to a net transport of water from cathode to anode, and the concentration of the two feed solutions needs to be rebalanced. (b) Some system components are expected to be more stable in contact with water than in contact with KOH solutions, and (c) because pure water is fed to commercial PEMEC systems, new AEMs and catalysts could be directly integrated into existing PEMEC systems if the feed remains pure water. It should be noted that the use of pure water will have an effect on the membrane resistance. Two opposing trends need to be considered: (a) an increasing KOH concentration increases the osmotic pressure difference, and thus reduces the water content of the membrane. (b) AEMs only exclude cations at very low concentrations [18] and absorb also potassium cations and additional hydroxide ions in, e.g., 1 M KOH solution. The first effect decreases the ion conductivity, and the second potentially increases the ion conductivity.

However, the use of pure water raises another issue: in alkaline systems, the feed solution itself is an excellent transport medium for hydroxide ions. In pure deionized (DI) water, membrane and catalyst particles need to be connected by a hydroxide conducting polymer. This ionomer binder could be the same polymer as the membrane polymer. In the ideal case, it is chemically similar, to allow low interfacial resistance and similar expansion in contact with water (to avoid delamination), but has a higher ion exchange capacity and higher permeability for hydrogen and oxygen, because the ionomer will partially coat the catalyst particles. Furthermore, the electrochemical stability of the polymers could be an issue. For example, some recent studies suggest that phenyl groups adsorbed on the catalyst surface get oxidized to phenols, which (because of the phenols' acidity) reduces the number of hydroxide ions. The solution would be phenyl group–free materials [19,20]. In direct contact with platinum catalysts, also the oxidation of organic cationic groups could be an issue [21].

1.3 Chemical Stability of Anion Exchange Membranes. AEM are much less stable under alkaline conditions than proton exchange membranes under acidic conditions. This is a major problem, which seriously hampers the development of AEM-based fuel cells and electrolyzers. Therefore, the low alkaline stability of AEMs has been researched intensively [21–23] and is now quite well understood. As shown in Fig. 1, hydroxide-induced degradation can occur at the backbone and at the functional group. The degradation of polymer backbones, leading to chain scission, decreases the molecular weight. This results in increased brittleness of the membrane and is especially pronounced in the presence of aromatic ether groups [24–26]. Therefore, this group, which unfortunately is present in many cheap and easily accessible polymers like PEEK, PESU, and polyphenylene oxide (PPO) should be avoided.

Degradation of the functional group does not necessarily affect the mechanical integrity of the membrane, but reduces the ion conductivity. For the most common functional group, quaternary ammonium ions, degradation mainly occurs by nucleophilic substitution reactions, in which hydroxide ions react either with a methyl group to methanol or with a methylene group to free trimethyl amine and a polymer bound alcohol group. Other discussed reactions are Hofmann elimination, which is only possible in the presence of β-hydrogen atoms (i.e., $C\mathbf{H_2}CH_2N(CH_3)_3$ and to a very minor extend Sommelet–Hauser and Stevens rearrangements [27].

It is still debated, how to evaluate the alkaline stability of AEMs. In simple ex situ tests, membrane samples are immersed in alkaline solutions. As a general trend, degradation seems to scale with the concentration of hydroxide ions in the membrane. High hydroxide concentrations are reached, when the membrane is not fully humidified, or when the solution in which the membrane is immersed has a high hydroxide concentration. The driving forces for the

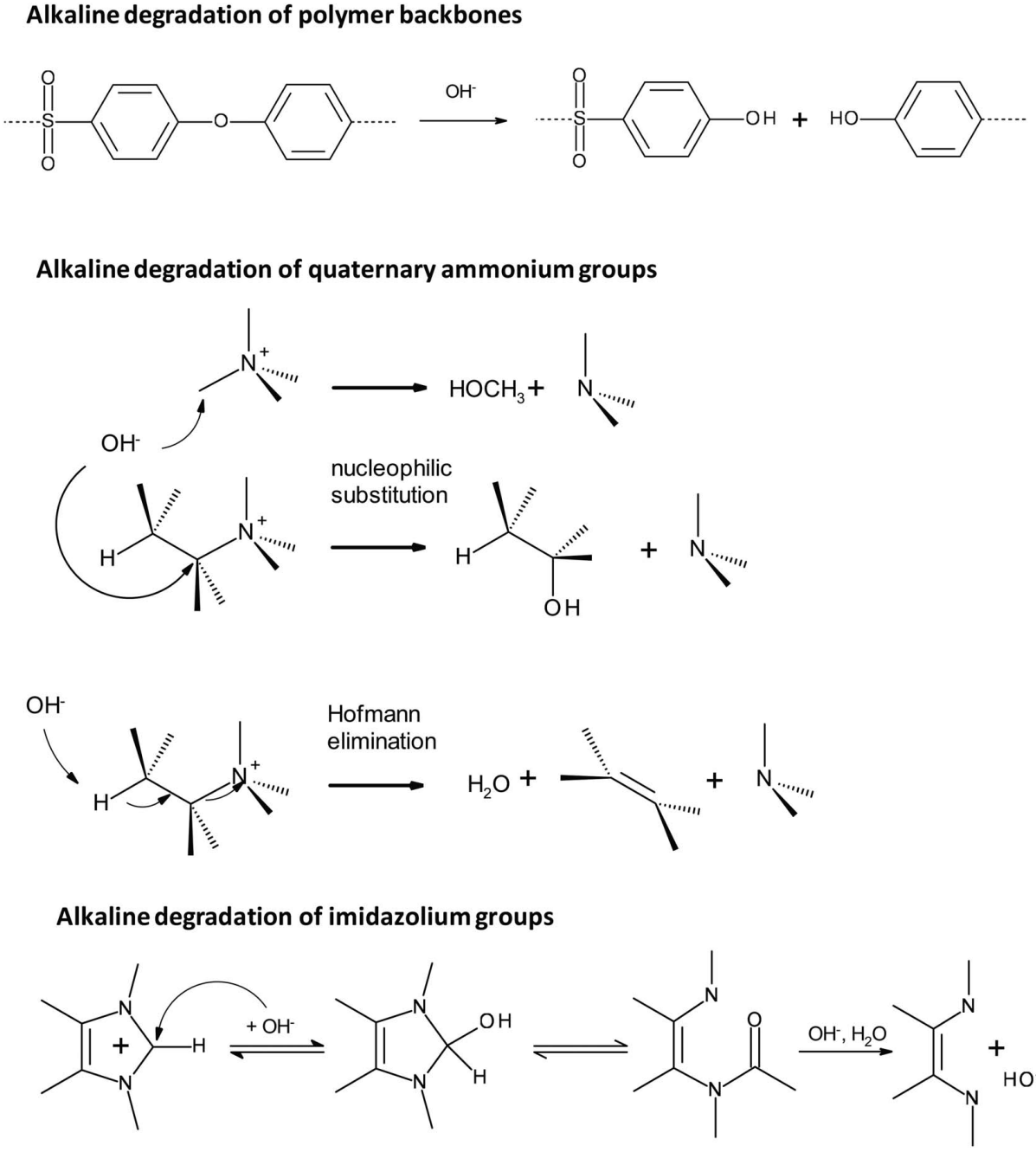

Fig. 1 Alkaline degradation of AEMs

accelerated degradation are that (a) hydroxide ions are less well solvated, and therefore more "naked," aggressive nucleophiles at low levels of humidification [28] and that (b) AEMs are not perfect single ion conductors but absorb also potassium ions and excess hydroxide ions when immersed in a KOH solution [18], increasing the number of reactive ions in the membrane. Furthermore, an increasing ion concentration in the outside solution (e.g., the feed solution) affects the osmotic pressure, which reduces the water absorption per absorbed hydroxide ion. Therefore, alkaline degradation of AEMs is expected to be higher in fuel cells than in water electrolyzers, and higher with alkaline feed solutions than with pure water. For electrolyzers, it can be deducted that situations where the membrane may not be fully humidified need to be avoided. Hypothetically, this could be a situation, in which the electrolyzer is operated with a "dry" cathode, and the rate of hydrogen production and removal of water with the hydrogen stream outpaces the transport of water, or a situation in which gas bubbles contact the membrane and absorb humidity from it.

In addition to the most common benzyl trimethylammonium groups, which are connected to aromatic polymer backbones via a methylene group, several other groups have been investigated like guanidinium [29], imidazolium [17,30,31], phosphonium [32], and cobaltocenium [33]. Guanidinium groups seem to be much less stable than standard benzyltrimethlammonium groups [34]. Some phosphonium groups showed promising properties, especially when the P atom has bulky substituents with a high electron density, like trimethoxyphenyl [32]. However, the molecular weight of these systems limits the ion exchange capacity (IEC). Since IEC is the number of functional groups per repeat unit/weight of the functionalized polymer repeat unit, the molecular weight of a monofunctional repeat unit should be <500 g/mol to reach an IEC >2 mmol/g. For comparison, the molecular weight of the functional

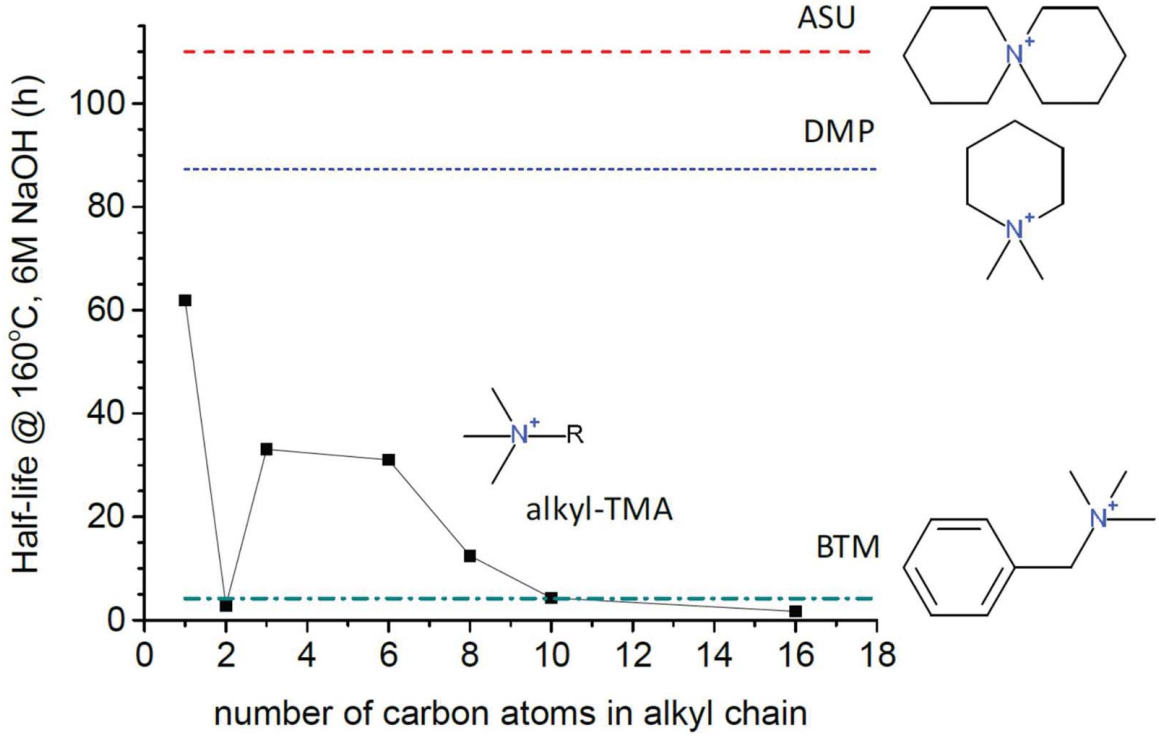

Fig. 2 Alkaline stability of model compounds: Marino and Kreuer obtained the half-life values by degrading the molecules in 6 M NaOH at 160 °C [34]

groups is 206 and 564 for cobaltocenium hydroxide and the described phosphonium group, respectively, but just 91 g/mol for tetramethylammonium hydroxide. An interesting group is imidazolium, which can be functionalized in all five positions. This allows us to sterically protect the labile C2 position against reaction with hydroxide ions, and to tune the electron density of the C2 position, resulting in quite different alkaline stabilities for different imidazolium structures [30].

A study with model compounds revealed that benzyltrimethylammonium (BTM), which represents the standard quaternary ammonium group in many publications, is less alkaline stable than methyl-trimethylamine (TMA) [34]. The reason is the negative inductive effect of phenyl substituents, which increases the positive charge on BTM (Fig. 2). This suggests that long alkyl chain tethered ammonium groups could be more stable than BTM. However, ethyl-TMA has a very low stability, because the β-hydrogen atoms participate in Hofmann elimination. Interestingly, the addition of another methylene group (propyl-TMA) again increases the alkaline stability, which then appears to remain constant up to hexyl-TMA and then declines again. The effect that stabilizes alkyl-TMA with alkyl chain lengths larger than ethyl is that the free rotation of the β-hydrogen-containing group is hindered by the additional CH_3 group. This slows down the Hofmann elimination, which proceeds via a conformation in which ammonium and β-hydrogen are in anti-conformation (Fig. 1). It is not clear what happens exactly at very long chain lengths above C6 or C7, but one effect could be micelle formation, at least in the case of model compounds. For AEMs, the density of functional groups and the rigidity of the polymer backbone very probably will also play a role. Another important observation is that some aliphatic heterocycles, especially ASU (6-azonia-spiro[5.5]undecane) and DMP (*N,N*-dimethylpiperidinium), show a much higher half-life in hot NaOH solution than BTM. The reason is that the conformations of the cyclic structures are energetically unfavorable for Hofmann elimination.

Another issue could be radical degradation, which is the main reason for chemical degradation in PEM fuel cells and electrolyzers. There, extreme care is taken to avoid contamination with transition metal ions like iron or nickel, which catalyze the degradation of peroxide (a by-product in fuel cells and electrolyzers) into reactive oxygen species like hydroxyl and hydroperoxyl radicals. To protect the membranes and ionomers, state-of-the art PEM fuel cell membranes contain now additives like cerium salts or oxides, which rapidly degrade peroxides into oxygen and water [35,36]. Because alkaline stability was in the main focus of researchers so far [21], it is not well investigated yet how much AEMs suffer from attack by reactive oxygen species. However, it is known that peroxides decompose rapidly in contact with NaOH [37,38], and it could well be possible that AEMs are relatively protected against peroxide-induced degradation by the high pH in AEM water electrolyzers. In addition, hydroxyl and hydroperoxyl radical are not formed under alkaline conditions [23]. However, in AEM-based fuel cells, the formation of superoxide radicals (O_2^{*-}) was recently reported [39]. Apparently, the reduction of oxygen with hydroxide ions, resulting in superoxide anion radicals and hydroxyl radicals, is catalyzed by quaternary ammonium groups [40]. Investigation into the stability of AEMs toward superoxide radicals and ways to mitigate them may become an important issue in the future.

1.4 Leads for Membrane Development. For most types of membranes, the quaternary ammonium groups are introduced by reaction of chloro- or bromomethyl groups bound to a polymer backbone with an amine, e.g., trimethylamine (TMA), *N*-methylmorpholine, or 1-methylimidazole. Based on the aforementioned, polymers should not have aromatic ether groups, because they were shown to react with hydroxides [24–26]. Purely aromatic polymer backbones have been developed, but their high rigidity may lead to brittle membranes and necessitates a high molecular weight [26,41]. Therefore, aliphatic or mixed aromatic/aliphatic backbones seem to be most promising [42]. Since radical degradation may be less relevant in alkaline conditions, polymers based on polystyrene, which fail fast in PEM fuel cells [43], can be considered. To

reduce the rigidity of polystyrene, block copolymers of styrene and ethane and butadiene, e.g., SEBS, can be used [44,45]. Another way to use polystyrene is to graft vinylbenzylchloride on electron beam or gamma-ray-irradiated films (polyethylene, ETFE, FEP, etc.), followed by amination [46,47].

A second polymer type is prepared by Friedel–Crafts reaction between aromatic monomers and aliphatic ketones, e.g., CF_3-CO-$(CH_2)_5$-Br [48,49]. The third class of polymer backbones is based on polybenzimidazole. Here, charged groups are introduced by methylation, resulting in ionenes, which carry the positively charged groups in the polymer chain [50–54], or by attaching charged groups to the polymer backbone [55,56].

To increase the dimensional stability and mechanical strength, membranes should be crosslinked, supported with a strong inert porous polymeric layer or nanofiber mat and/or reinforced by the addition of fillers. The latter has the potential advantage that gases need to diffuse around the added nanoparticles, and the increased tortuosity reduces the permeability for gases [57].

2 Targeted Properties for Anion Exchange Membrane Water Electrolysis Membranes

The target values displayed in Table 1 are based on a recent call for proposals (EU Horizon 2020) [58], and therefore should not be understood as universally accepted values, but more as a guidance. Especially, lower performances in one parameter could be compensated by better performance in another parameter. For example, a highly stable system could be preferred over a less stable, but more efficient system. Also, a poor ion conductivity could be compensated by a low-area-specific resistance (ASR).

ASR and through-plane ion conductivity are related by the thickness according to the equation

$$\text{Ion conductivity (mS cm}^{-1}) = \frac{\text{Thickness}}{\text{ASR } (\Omega\ \text{cm}^2)},$$

$$\text{ASR} = \text{Membrane resistance} \times \text{Area}$$

To achieve both targets of (a) ASR of 0.07 $\Omega\ \text{cm}^2$ and (b) ion conductivity of 50 mS cm^{-1}, the maximum membrane thickness is 35 μm. If the ion conductivity is doubled to 100 mS cm^{-1}, the maximum thickness is 70 μm.

Thin membranes are technically possible, but hydrogen crossover increases and mechanical stability decreases with decreasing thickness. It is interesting that gas permeation was not mentioned in the call conditions, because hydrogen crossover is a common key performance indicator and most relevant for safe operation. On the other hand, safe operation can be assumed when the concentration of hydrogen is below 2% (4% is the lower explosion limit), and since this low hydrogen concentration can be reached by increasing the membrane thickness, the ASR target value in combination with the concentration limit of 2% H_2 in O_2 indirectly controls the maximum permissible permeability.

Table 1 Target specifications for AEM in the NEWELY project, based on the call conditions (EU Horizon 2020/Fuel Cells and Hydrogen Joint Undertaking (JU), call FCH-02-4-2019)

Parameter	Target value	Comment
Ion conductivity	>50 mS cm^{-1}	At room temperature, hydroxide form, in DI water or close to 100%rh
Area-specific resistance (ASR)	≤0.07 $\Omega\ \text{cm}^2$	ASR = thickness/ion conductivity
Stability	≤0.07 $\Omega\ \text{cm}^2$ after 2000 h real or simulated operation in an electrolyzer	Predicted time, in situ or ex situ DI water/100%RH, 0.1 M KOH or 1 M KOH
Tensile strength	>15 MPa	
Elongation at break	>100%	
dry/wet dimensional stability	≤1% in machine direction ≤4% in transverse direction	

At first glance, mechanical properties may appear to be less important for AEMWE, because there are no movable parts, and different from fuel cells, the hydration level of the membranes is expected to be constant. However, four scenarios need to be considered:

(1) Situations, in which the feed water is removed from the cell, either for maintenance or by accident;
(2) in the case of membranes assembled with catalyst-coated porous transport layers, air bubbles may contact the membrane, leading to local differences in absorbed water;
(3) the most important issue, as further discussed after the next paragraph: large pores in the porous transport layer can damage the membrane, which is pressed into these pores at differential pressures or during pressure fluctuations; and
(4) the most common scenario: water absorption of AEM increases with the temperature; during the start-up of AEMWE, the temperature increases from room temperature to 50 or 60 °C. This swells the membrane, leading to wrinkles, and in the case of catalyst-coated membranes, possibly to delamination of membrane and catalyst layers. During shutdown, the membranes will lose water and shrink, leading to mechanical stresses. This swelling and shrinking effects especially the parts of the membranes at the interface between the active and the inactive areas, because the active and inactive areas of the membrane respond differently (the inactive area is clamped between the gaskets) and at different times (the inactive area will respond with a delay) to changes in the operating conditions [59].

Electrolysis operation at differential pressure seems to be the ideal operational mode: A high cathode pressure reduces the costs for mechanical hydrogen compression and reduces the water content in the hydrogen stream and thus the cost for drying. Furthermore, a low anode pressure reduces the oxidative potential of pure oxygen. The major disadvantages are increased gas crossover and mechanical damage to the AEM. For simplicity, many researchers test their cells at ambient pressure, and the apparent stability can be very misleading for the following development steps toward differential pressure.

To prevent wrinkling at operation conditions and mechanical damage, it is recommended to assemble electrolysis membranes in the wet state [60]. However, this is usually not done in research, presumably because membranes lose water rapidly in ambient atmosphere, and handling under water or in humidified air is complicated. Therefore, while a high mechanical strength is wanted, perhaps even more relevant could be a high-dimensional stability, which eliminates detrimental in-plane swelling/shrinking. One potential alternative could be to use the shape memory effect of membranes, which is programmed when they dry under a fixed geometry. As shown for Nafion 212 and a radiation-grafted PEM, such membranes swell preferentially in the thickness direction when re-humidified. When these membranes are assembled in the dry state into a fuel cell, they remain free of folds and wrinkles when humidified, and the memory effect is re-established when the membranes shrink again, because membranes are clamped tightly between the bipolar plates, restricting shrinking in the area [61,62]. Ultimately, because swelling in the thickness will increase the contact between the membrane and the porous electrode, the total swelling should be as low as possible.

3 Commercially Available State-of-the Art Membranes

Membranes of anion exchange resins have been developed for over 70 years [63]. However, because of the low alkaline stability

Table 2 Commercial AEMs and their reported properties

Brand name	Company	Country	Product code	Thickness (μm)	IEC (meq/g)	Ion conductivity (mS cm^{-1})	ASR (Ω cm^{2})	Dimensional stability (%)	Tensile strength (MPa)	Elongation at break (%)
Fumasep® FAA3	Fumatech	Germany	FAA-3–30	25–35[a]	1.7–2.1 (Cl)[a]	4–7 (Cl)[a] 40 (OH) [67]	0.3–0.5 (Cl)[a]	0–2 (Br)[a]	25–40[a]	20–40[a]
			FAA-3-50	47–53[a]	1.85[a]	as above	<2.5(Cl)[a]	as above	as above	as above
			FAA-3-PK-75	75[a]	1.39 (Cl)[a]	>2.5 (Cl)[a]	<2.0 (Cl)[a]	0 (Br)[a]	20–45[a]	30–50[a]
A201	Tokuyama	Japan	A201	28 [68]	1.8 [68]	42 (OH) [68]	Na	2 (MD) [68] 6 (TD) [68]	96 (dry, Cl) [69]	62 (dry, Cl) [69]
AEMION™	Ionomr	Canada	AF1-HNN8-50-X	50[a]	2.1–2.5[a]	>80[a]	0.13[a]	na	60 (dry, I)[a]	85–110 (dry, I)[a]
			AF1-HNN8-25-X	25[a]	2.1–2.5[a]	>80[a]	0.063[a]	na	60 (dry, I)[a]	85–110 (dry, I)[a]
			AF1-HNN5-50-X	50[a]	1.4–1.7[a]	15–25[a]	0.42–0.67[a]	na	60 (dry, I)[a]	85–110 (dry, I)[a]
			AF1-HNN5-25-X	25[a]	1.4–1.7[a]	15–25[a]	0.21–0.33[a]	na	60 (dry, I)[a]	85–110 (dry, I)[a]
SUSTAINION®	Dioxide Materials	USA	Sustainion 37–50	50 [17]	na	80 (1 M KOH, 30 °C) [17]	0.045 (1 M KOH) [17]	cracks when dry	cracks when dry	cracks when dry
Orion TM1	Orion Polymer	USA	Pure material m-TPN1 [48]	24 [48]	2.19(OH)[a]	19 (Cl) [48] 54 (OH) [48] >60[a]	na	6 (Cl) [48] 10 (OH) [48]	30 [48]	35 [48]

[a]From technical data sheet.

of the earlier membranes, most membranes were optimized for chemically less aggressive environments, like desalination, electrodeionization, or electrodialysis [22]. While there have been early reports on AEM-based fuel cells [64], work on AEM water electrolyzers started relatively late [15,65]. Therefore, although there are many other membrane companies and membranes, e.g., from Asahi Chemical Industry, AGC, Mega, Solvay, Tianwei Membrane Technology and Membranes International, Table 2 only lists a selection of those membranes which have been mostly investigated for their use in AEM water electrolyzers. Also, the table does not show the properties of all available membranes or membrane grades; usually, more membranes are available upon request, differing in thickness or having a porous support or other reinforcements.

Diaphragms like AGFA's Zirfon [2] or ion-solvating membranes (e.g., polybenzimidazole) [66] can only be used in alkaline water electrolyzers and are therefore not considered here.

It should be pointed out also that the conductivity values cannot be exactly compared. Some producers (e.g., Fumatech) measure the hydroxide conductivity by immersing membranes first in KOH solution to achieve full ion exchange (which may not be complete) and then changing the solution to pure water, to leach out excess KOH. This should be done in a closed system using nitrogen purged water, or in a glove box to prevent contact of the membrane with CO_2 [70], but the exact process is usually not reported. Another method is to electrochemically purge carbonates from the membrane by applying a voltage in a CO_2-free atmosphere. Values obtained in this way are significantly higher than those measured with the first method and are more close to the conductivity observed in an operating electrolysis cell [71,72].

Another important property is the permeability for hydrogen and oxygen. Since the permeability depends on various factors (temperature, water uptake, carbonate or hydroxide form, etc.) and is seldom reported, permeability coefficients are not included in Table 2. However, some values are available: in contact with 1 M KOH, an FAA3 membrane showed a hydrogen permeability at 50 °C of $7.3 \cdot 10^{-17}$ mol(cm · s · Pa)$^{-1}$ [73]. For oxygen, a permeability of $4.0 \cdot 10^{-13}$ mol(cm · s)$^{-1}$ at 60 °C and 98% relative humidity was reported [74]. For A201, a hydrogen permeability at 50 °C of $5.3 \cdot 10^{-17}$ mol(cm · s · Pa)$^{-1}$ was measured [73] and an oxygen permeability at 20 °C of $3.9 \cdot 10^{-17}$ mol(cm · s · Pa)$^{-1}$ [75]. By measuring the hydrogen concentration in the anode compartment, Ito et al. were able to provide in situ values. For an electrolyzer equipped with A201, the hydrogen permeability was $5.6 \cdot 10^{-17}$ mol(cm · s · Pa)$^{-1}$ [76]. Interestingly, this was just one-fifth of the value measured in a PEM system. However, measuring in situ measured values usually does not account for the potential reaction of hydrogen and oxygen to water, so that the real crossover values could be somehow larger. For Aemion (HMT-PMBI in the hydroxide form), an ex situ oxygen permeability of $2.0 \cdot 10^{-12}$ mol(cm · s)$^{-1}$ at 60 °C and at 98% relative humidity was observed [74].

Another parameter which is not mentioned in Table 2 is the water permeability. In systems where pure water is fed to both electrodes, this seems to be of low importance, because water is replenished continuously and can be balanced easily between the two sides. However, it can be advantages to operate an AEM water electrolyzer so that pure water is fed only to the anode chamber [77]. This operation mode reduces the risk that gas bubbles block the catalyst layers and reduces the amount of water carried away by the gas stream. The first effect increases the performance, and the second reduces the efforts to dry the hydrogen stream. If water transport from anode to cathode by permeation through the membrane is too slow to compensate the consumed water and water transported away by electro-osmotic drag (hydroxides move from cathode to anode) and the hydrogen stream, mass transport losses are expected. The more probable scenario, however, is that too much water is transported through the membrane. This not only increases the humidity of the hydrogen stream, but also can flood the cathode [78]. Vapor/vapor fluxes of FAA3-30, FAA3-PK-75, and Tokuyama A201 were reported to be 15.1, 12.7, and 21.3 mmol m^{-2} s^{-1}, respectively, at 70 °C and a humidity gradient of 100%/50% [69]. The water permeability of FAA3 and HMT-PMBI (the basis of Aemion membranes) was analyzed in detail by Luo et al. [79]. The most relevant water/vapor fluxes at 70 °C for a gradient of water/50% were reported to be 12 mmol m^{-2} s^{-1} for FAA3 and 15 mmol m^{-2} s^{-1} for HMT-PMBI, both in the carbonate form. For the hydroxide forms, which usually absorb more water than the carbonate form, higher fluxes are expected.

The mechanical properties are usually reported for well-controlled conditions; that usually is the dry halogenide form at room temperature. The relevant wet hydroxide form at elevated temperature cannot

be analyzed, unless the stress–strain measurement is done in an inert, temperature- and humidity-controlled atmosphere. Therefore, the data in the literature usually do not report on those properties which are really of interest. In general, a high tensile strength, high Young's modulus, and high elongation at break are wanted. The latter could be somehow favored, because a flexible membrane will yield to the stress and needs substantial strain before it cracks.

3.1 Fumatech: FAA3. This membrane is available through Fumatech and independent distributors, and can be provided in many different thicknesses as non-supported or PEEK- or PP-reinforced membrane. The cost for a 20 cm × 30 cm sheet is currently one of the lowest among the discussed membranes. But this could change, if another company would scale up the production.

Chemically, FAA3 is a polyaromatic polymer with ether bonds in the main chain, and quaternary ammonium groups attached to the main chain. While old membranes (2011) were not crosslinked, newer membrane batches are slightly crosslinked. For the use as ionomer, also fully soluble linear polymers are available. In one work, it was observed that the Fumion FAA3-ionomer flakes formed a gel phase in dimethylacetamide (DMAc). The addition of a small amount of trimethylamine to the solution prevented gelation [78].

A water electrolysis cell operating with FAA3-50 and a 1 M KOH feed, and with Pt/C and IrO_2 as catalyst achieved a current density of 1.5 A cm^{-2} at 2.0 V (50 °C) and 1.9 V (70 °C) [16]. In another work, which focused on the electrode fabrication, a cell with FAA-3-PK-75 was operated at 1.8 V, resulting in current densities of 460 (50 °C) and 625 (70 °C) mA cm^{-2} [80]. In terms of the life time, a non-reinforced FAA3-40 membrane failed within 31 h because excessive swelling led to poor mechanical stability, while a PP-reinforced FAA-3-PP-75 membrane showed an initial voltage increase but then operated stably for the remaining 150 h of test [81]. In other systems, the non-supported FAA3-50 membrane was shown to operate stably for 1000 h [82].

3.2 Tokuyama: A201. Tokuyama's AEM were only available through Tokuyama, and purchase required signing a non-disclosure agreement. Unfortunately, this product is discontinued. The structure of Tokuyama A201 (which is different from the older Aciplex A201) and that of the chemically same but thinner (11 μm) A901 membrane are not disclosed, except that they are hydrocarbon-based membranes with quaternary ammonium groups.

An electrolyzer equipped with a Tokuyama A201 membrane was operated with carbonate solution for 1000 h. While the cell voltage at 470 mA cm^{-2} slightly increased from ca. 1.9 V to 2.05 V, the cell resistance remained even more stable, indicating that the membrane did not degrade significantly [83]. In 1 M KOH solution at 80 °C, the ion conductivity (after exchanging back into the chloride form) did practically not vary over a time of 14 days [69].

3.3 Ionomr: AEMION. Ionomr currently offers four standard membranes, which vary in IEC (1.4–1.7 or 2.1–2.5 meq/g) and thickness (25 or 50 μm). They can be obtained directly from the producer.

Aemion membranes were developed in the Holdcroft group at Simon Fraser University and are based on methylated polybenzimidazoles. Degradation of methylated polybenzimidazole (PBI) starts from attack of hydroxides on the C2 position of the imidazolium moiety [50,51]. In Aemion membranes, this attack is sterically hindered by the introduction of methyl groups in both *ortho*-positions of the linking 2-phenyl group [52]. The alkaline stability can be further improved by increasing the electron density on C2. This can be achieved by changing the linking 2-phenyl group for a larger system, so that the positive charges of two neighboring imidazolium ions are not stabilized by one phenyl ring, but by at least two phenyl rings [53,54]. Although the exact structure is not disclosed, one exemplary structure is that of HMT-PDMBI (Fig. 3) [84,85].

The research-based HMT-PDMBI membrane was tested in an AEM water electrolyzer. With a NiAl anode and a NiAlMo cathode and a 1 M KOH feed, the cell delivered 1 A cm^{-2} at a stable voltage of 2.1 V for over 150 h [86]. Recently, also all four membranes in IONOMR's portfolio were tested in AEM water electrolyzers in 1 M KOH at 50 °C [87]. The best performing membrane was AF1-HNN8-25-X. A current density of 500 mA cm^{-2} was obtained at 1.7 V and showed a voltage increase of 2.4 mV h^{-1} over the tested 17 h. This is significantly higher than the state-of-the art (5 μV h^{-1}) [88], but impedance spectroscopy revealed that the source for this degradation was severe catalyst degradation: the resistance of the membrane did not increase [87].

3.4 Dioxide Materials: Sustainion. Sustainion samples can be obtained directly through dioxide materials and independent distributors. Dioxide material's sustainion membranes were developed in Richard Masel's group and are based on a classic poly(4-vinylbenzyl chloride-co-styrene) chemistry (Fig. 4) [17,31]. The structural design seems to be influenced by Weber et al.'s work (1-methyl imidazole functionalized poly(vinylbenzyl chloride) [89]) and Hugar et al.'s finding that 1-benzyl-2,3,4,5-tetramethylimidazolium groups are the most alkaline stable in a series of 1-benzyl imidazolium ions [30].

The product code Sustainion 37–50 seems to indicate the molar ratio of 4-vinylbenzyl chloride in the copolymer (37%) and the thickness (50 μm). Although the synthesis is done under nitrogen atmosphere, it was reported that trace water is actually wanted to produce crosslinked structures which show reduced swelling [90]. As expected for polystyrene based polymers, the material is rather brittle and cracks easily in the dry state. Therefore, dioxide materials ship Sustainion membranes as a "classic Sustainion" containing a water-soluble plasticizer, and as "Class 60 Sustainon" with a reduced amount of this plasticizer, which needs to be washed out from the assembled electrolysis cell with the first feed water. Probably for operation at higher pressure, dioxide materials also offer a polytetrafluoroethylene (PTFE)-supported "Class T Sustainion" and a "Class TZ Sustainion," which contains a PTFE support and is reinforced with zirconium oxide nanoparticles.

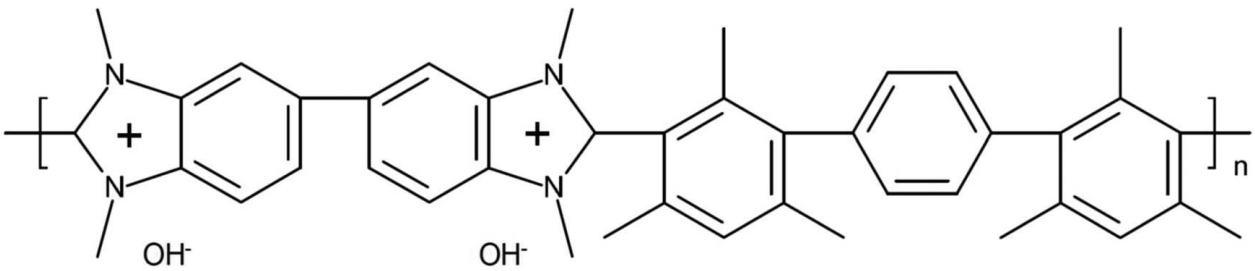

Fig. 3 Structure of HMT-PDMBI (hexamethylterphenyl-polydimethylbenzimidazolium)

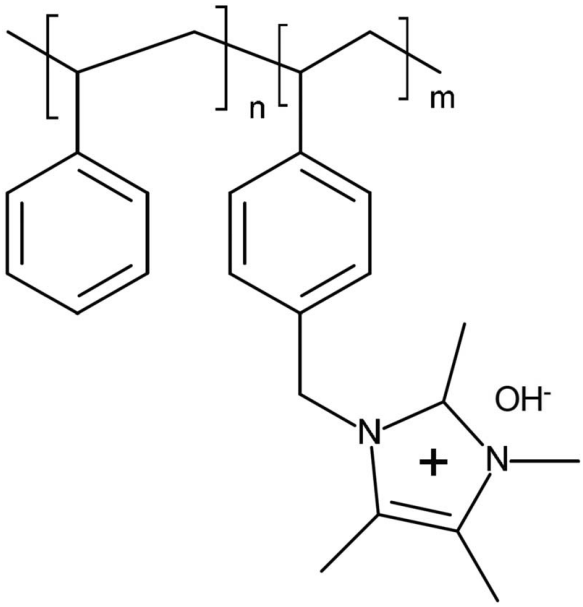

Fig. 4 Structure of Sustainion membranes [91]

Although very stable performances were demonstrated, the low alkaline stability of imidazolium ions and the fact that no data for operation in pure water are available raises the question if Sustainion perhaps is in fact not a real AEM, but conductive because of absorbed KOH and water. Although this may play a role, Hugar et al. showed that 87% of 1-benzyl-2,3,4,5-tetramethyl-imidazolium ions were retained in 1 M KOH/deuterated methanol at 80 °C after 30 days, whereas >99% of 1-methyl-3-benzyl imidazolium derivative was degraded under these conditions [30].

In a water electrolysis test, a cell with Sustainion 37–50 membrane and $NiFe_2O_4$ anode and NiFeCo cathode catalysts showed a stable performance of 1 A cm^{-2} at 1.9 V for over 2000 h [17]. With PGM catalysts, even 2 A cm^{-2} at 1.7 V were achieved, which seems to be the best reported performance so far for commercial membranes [91].

3.5 Orion Polymer: Orion TM1. Orion Polymer's TM1-based membranes are available now in three grades, non-reinforced membranes with an IEC of 2.19 meq/g, and 5–50 μm thick reinforced membranes optimized for use in applications. Samples can be obtained through the producer and independent distributors.

TM1 membranes were developed by Chulsung Bae's group at the Rensselaer Polytechnic Institute [48]. The synthesis of these membranes seems to be simple and easily scalable. However, the monomer 7-bromo-trifluorheptanone appears to be relatively

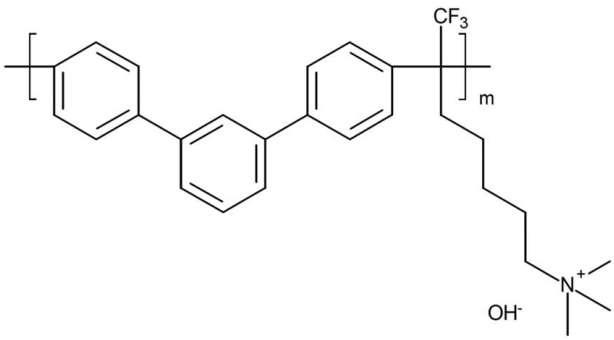

Fig. 5 Structure of Orion TM1

expensive (8 USD/g was the cheapest offer we found). The chemical structure was rationally designed: to avoid backbone degradation, the backbone does not contain aromatic ether groups (Fig. 5), which were identified to be the source of membrane failure in other AEM [24]. By connecting rigid aromatic systems by substituted methylene linkers, the flexibility of the polymer chains is enhanced, allowing for well-soluble polymers and good handling of the membranes. The length of the linking chain, to which the quaternary ammonium group is attached, was chosen within a certain length, because longer chains offer some steric protection and mobility of the cationic group, enhancing alkaline stability, phase separation, and ion conductivity [34,92]. In a recent survey conducted by the National Renewable Energy Laboratory (NREL), over 50 AEM from over ten organizations were tested for their alkaline stability. Orion TM1 was the most stable membrane in this test, and the only membrane which did not show signs of degradation [93]. In the AEM water electrolyzer, the TM1 (TPN1-100 in the scientific literature) showed a stable initial performance, but suffered from low mechanical stability in the hydrated state [94].

3.6 Performance of Commercial Membranes in Anion Exchange Membrane Water Electrolyzers. What remains relatively rare in the literature is information on the performance of cells based on these membrane types. This is despite the fact that only cell tests can verify the suitability of the membrane (conductivity, thickness, mechanical and chemical stability, and permeability to hydrogen) and ionomer itself (binder) for this specific application. The performance is connected with the membrane's interaction with the complementary cell components (porous transport layer, catalyst, and circulating medium), as well as with the compatibility with the cell design and operational conditions (feed composition, flowrate, and temperature) used. Table 3 (in the Appendix) summarizes the results reported for the mentioned commercially available AEMs in open sources. It includes key components, operation conditions, and performances of AEM water electrolyzers. This table, unfortunately, documents one important fact. AEM water electrolysis is currently importantly underdeveloped and even a generally accepted standardized testing protocol allowing for reliable comparison of different materials available/newly prepared does not exist.

Due to the aforementioned facts, it is difficult to organize systematically and to understand the results reported holistically. Different criteria may be used to achieve this target, e.g., type of catalyst (PGM versus non-PGM), circulating medium (KOH solution versus carbonate solution versus demineralized water), binder of catalytic layer (ionomer versus PTFE), or operating temperature (below versus above 50 °C). Figure 6 visualizes the basic trends observed in Table 3. It compares the highest current densities achieved at the cell voltage of 1.8 V with respect to the selected parameter. In the first case, it is the anion-selective membrane manufacturer and the catalyst type. In the second case, the circulating medium and catalytic binder type are addressed.

The first obvious conclusion derived from Fig. 6(*a*) is that cells utilizing PGM catalysts outperformed cells utilizing non-PGM catalysts. This finding was expected. Just in the case of the Tokuyama membrane the difference was not as significant as in the remaining cases. This can be explained by the fact that the mass transport strongly depended on the circulating solution (non-conductive PTFE was used in the catalyst layer for both PGM and non-PGM cells), and the concentrations of the used liquid electrolytes were different. The KOH concentrations were 0.1 and 1 M for PGM and non-PGM cell, respectively [83,95]. A combination of these two factors could lead to better utilization of the non-PGM catalyst due to improved ionic contact in the catalyst layer. Thus, the cell utilizing non-PGM catalyst exhibited a current density close to that of the cell with PGM catalyst.

This observation stresses the importance of the role of the anion-selective polymer binder when deionized water (or highly diluted alkaline solutions) is utilized as the circulating medium. It can be

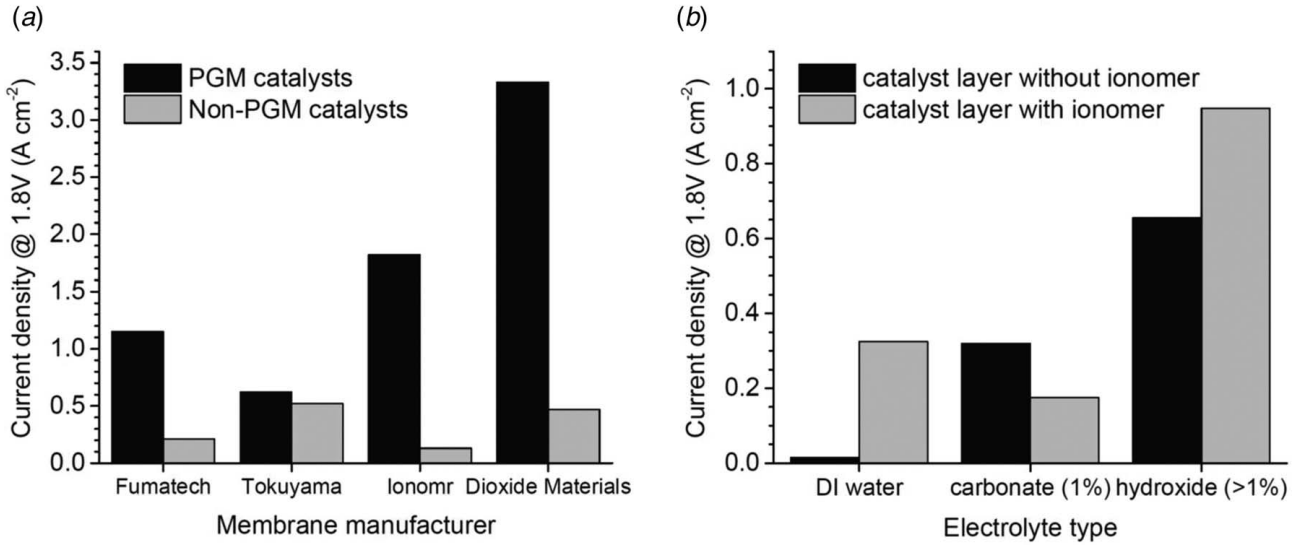

Fig. 6 Comparison of (*a*) the highest current densities observed for selected AEM manufacturers (indicated in the *x*-axis description) [16,17,69,82,88,93,97,98] and (*b*) average current densities observed for electrolyte type (indicated in the *x*-axis description) @ 1.8 V cell voltage in alkaline electrolytes. Orion membranes are not included, because the data base is too small yet.

further documented by the example of the Fumatech membrane, where the data are available [96,97]. Utilizing a non-PGM catalyst and an anion-selective polymer binder, it was possible to achieve significantly higher current density (0.25 A cm^{-2} @ 1.8 V) [97] when compared to a cell based on PGM catalyst with inert PTFE binder (0.02 A cm^{-2} @ 1.8 V) [96]. The influence of the polymer binder in context of the circulating medium composition is documented in Fig. 6(*b*).

Several conclusions can be derived from Fig. 6(*b*). At first, it is obvious that the utilization of DI water as circulating medium is possible only if an anion-selective polymer binder is applied. In that case, cell performance is comparable to that with carbonate-based circulating medium. This indicates that a comparable ionic contact between the catalyst and AEM is obtained for cells with ionomer binder and cells with inert binder/1 wt% carbonate solution. Interestingly, the average performance was improved even in the case of the hydroxide solution if an anion-selective polymer binder was applied. This is clearly connected with improvement of the above-mentioned ionic contact to the membrane. This is explained by following aspects: (i) the active volume fraction of the hydroxyl conductive phase increases if the catalytic layer is soaked with KOH solution and (ii) the conductivity of the ionomer binder is increased as well due to complete conversion to the hydroxide form and absorption of additional potassium and hydroxide ions in the ionomer phase (Donnan exclusion is ideal at very diluted concentrations [18,99]). Figure 6(*b*) also shows that it is possible to achieve current densities up to 1 A cm^{-2} @ cell voltage 1.8 V in the case of the studied commercial membranes using hydroxide solution of 1 M KOH. This is in detail documented in Fig. 7.

Figure 7 documents that alkaline solutions clearly dominate as a circulating medium. As already discussed, the reason consists in improved ionic contact inside the cell and in stabilization of performance with regard to potential cell carbonization.

The line in Fig. 7 represents the performance of a typical current commercial PEM water electrolyzer [98]. It is thus a current target line for the AEM water electrolysis. However, the performance of commercial PEM electrolysis is improving, and the target line should not be mistaken as a static, unchangeable target. Furthermore, for AEM to reach market maturity, also the overall cost needs to be equal or better than that of PEM technology, and the stability must be sufficient. Even now some AEM systems clearly outperform the target line in Fig. 7. One recently reported AEM water electrolyzer using con-commercial membranes and ionomers, water as feed and NiFe/PtRu as catalyst reached 2.7 A cm^{-2} at 1.8 V [19]. However, this system was optimized for performance, and the authors caution that the durability needs to be improved.

Clearly, all cells outperforming the PEM system use a feed of 1 M KOH. But ultimately, pure water should be used, to ease the transfer of AEM technology to existing PEM electrolysis systems, but also to alleviate issues of rebalancing of the feed concentrations. The last aspect is connected with the fact that 2 mol water is consumed at the cathode and 1 mol water is produced at the anode per unit reaction. Another observation is that most data points above the target line, with only one exception, were obtained with platinum group metal (PGM)-containing catalysts.

Whereas the quality of ionic contact between catalyst layer and AEM impacts predominantly polarization voltage losses, membrane resistance is related directly to the ohmic losses of the cell. Therefore, the reported performance of the cells is significantly influenced by the membrane thickness [88] and operating temperature [80]. The role of membrane thickness is clear, as membrane ohmic resistance can be considered to be a linear function of its thickness. The reduced thickness of the AEM thus results in better performance of the cell [87]. At the same time, however, permeation of hydrogen through membranes increases. Additionally, AEMs with low thickness can be less mechanically stable under the conditions of the alkaline water electrolysis [81]. The typical solution of this problem represents the utilization of a suitable reinforcement by a porous support, e.g., a fabric or non-woven material. Reinforcement, on the other hand, reduces the conductive volume fraction of the membrane and thus increases its ohmic resistance. Reinforcement utilization thus represents a trade-off between membrane mechanical stability and performance.

Increasing temperature clearly improves ionic conductivity (Fig. 8). When considering the reported data, however, it is important to remember the fact that most membranes are not long-term stable at temperatures exceeding 50 °C and that therefore lower operating temperatures with lower performances may be preferred considering the enhanced durability. As a rule of thumb, the van't Hoff rule states that the speed of chemical reactions (e.g., alkaline degradation) at least doubles when the temperature is increased by 10 °C.

Recently, Bender et al. compared the literature-reported performances of PEM water electrolyzers [101]. The voltages at

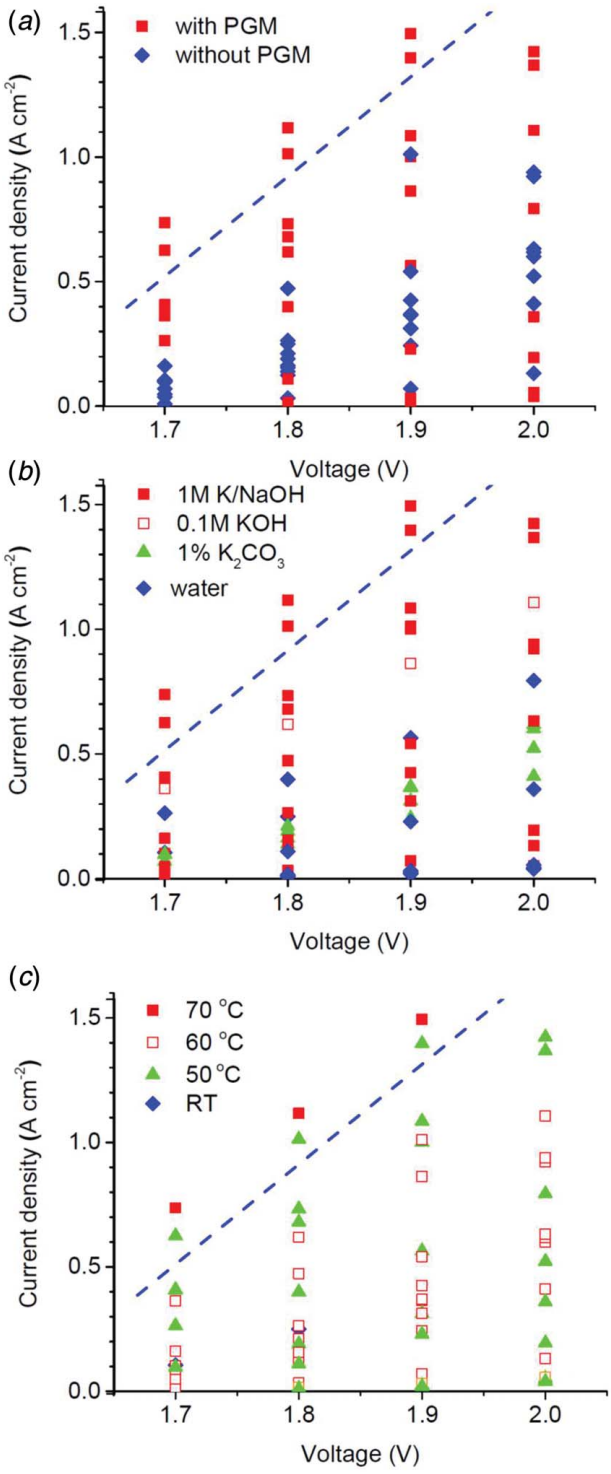

Fig. 7 Performances of AEM water electrolysis systems: (*a*) based on the use of PGM or non-PGM catalysts, (*b*) based on the feed, and (*c*) based on the operation temperature. The dotted line represents the performance of a commercial PEM water electrolysis system [98] and therefore indicates a current performance target for AEM water electrolyzers with pure water as feed. The reader is referred to the online version for color coding.

1 A cm^{-2} varied significantly and showed a deviation of 500 mV for Nafion 115 (based on 23 publications) and 600 mV for Nafion 212 (based on ten publications). In a round robin test, in which four labs used the same equipment and procedure, the average voltage at 1 A cm^{-2} was 1.787 V with a standard deviation of 0.010 V.

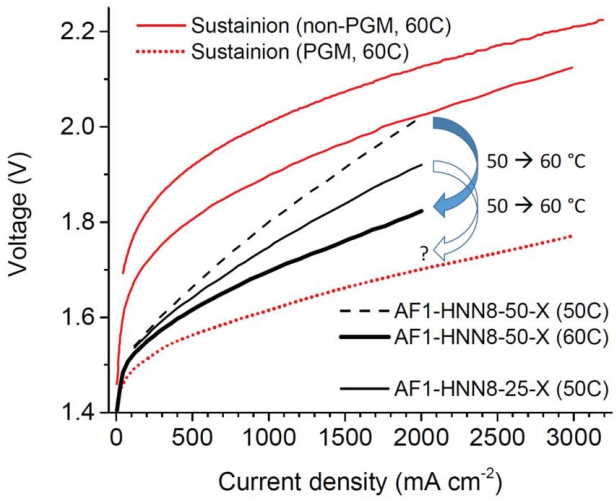

Fig. 8 Performance of AEM electrolyzers using Sustainion and Aemion membranes, all with 1 M KOH feed solutions [17,87,91,100]. The upper line is from Ref. [100], the lower lines for Sustainion are from Ref. [91]. Aemion membranes were tested with PGM catalysts, and Aemion ionomer at 50 °C and FAA3-ionomer at 60 °C. The question mark indicates that the performance of AF1-HNN8-25-X was not reported for 60 °C with FAA3 ionomer, but one may expect that it would be close to that of Sustainon. More data are needed for a final evaluation.

According to the authors, the temperature control was the most significant source for the observed deviation. For the AEM water electrolysis, the expected variation of the literature values must be even larger, because tested systems vary also in the composition of the feed solutions. Another potential issue is the batch-to-batch reproducibility. Pristine TM1 (Orion) can be expected to have a low variability of the IEC value, because the IEC is fixed by the chemical structure. The same is true for Sustainion, in which the IEC depends on the composition of the monomer feeds, which can be well controlled. However, since Sustainion is known to be mildly crosslinked by reaction of water traces with the benzylchloride groups, the degree of crosslinking and thus the swelling and conductivity could vary. For Fumatech membranes, the specified IEC varies between different batches. For example, we received batches for

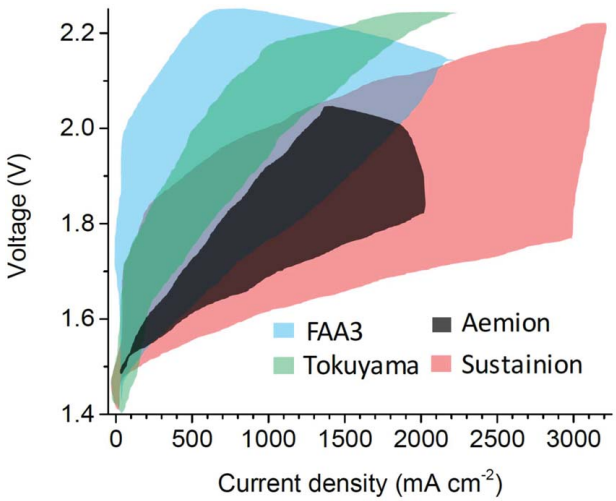

Fig. 9 Performance range of AEM water electrolyzers using different membranes and different operating conditions. Orion TM1 Durion membranes are not included because not enough literature is yet available (we are only aware of one report (Table 3)).

which the IEC was specified as 1.63, 1.7–2.1, and 1.85 meq/g. This could indicate changes in the product specification over the years, but could also indicate that the synthesis of FAA3 includes a bromination or chloromethylation step, which is difficult to control. Similarly, Aemion is prepared by the methylation of PBI, and the degree of methylation may vary. In case a tight specification is requested by customers, companies can reach these values also by blending batches with low and high values. This is common practice in some industries (e.g., commodity polymers may show bimodal molecular weight distributions for this reason), and for AEM could affect other properties, like crystallinity and mechanical properties. Finally, while chemical properties can be well characterized for each batch, the way membranes are produced in large scale, typically by casting a polymer solution on a moving support belt or film, makes it difficult to guarantee that all membrane properties are exactly the same at (for example) roll meter 5 and 18, due to fluctuations in temperature, casting thickness, residual solvent content, etc. Therefore, in any case, customers are recommended to look closely at the specifications when ordering AEMs, and to check individual samples at least for their wet thickness before use.

A comparison of cell performances based on individual commercially available membranes is shown in Fig. 9. The overlay of the discussed data suggests that the performances of commercial membranes can be sorted into two groups: Fumatech and Tokuyama membranes (hydroxide conductivity in the range of 40 mS cm^{-1}, Table 2) appear to have a lower performance, and the newer membranes Aemion and Sustainon (conductivity up to 80 mS cm^{-1} in the best grades) have a higher performance. However, as discussed earlier, higher ionic conductivity can have a negative impact on the other characteristics of the electrolysis cell, particularly on the penetration of H_2 to the O_2 stream, especially under differential pressure conditions. Unfortunately, due to the novelty of the Aeminon and Sustanion membranes, these values are not yet specified in scientific literature. To define a "winner" between these membranes requires significantly more work. Additional data have to be collected. This is especially true when considering operation with deionized water as a circulating medium. At the same time, it can be said that there is still sufficient space for improvement in order to outperform PEM water electrolyzers.

3.7 Stability. The most pressing issue is the stability of AEMs, which is limited by chemical and mechanical degradation. However, most work only focuses on the initial performance after cell activation, and in the best cases, 2000 h of operation for Sustainion [17] and 1000 h for A201 [83] and FAA3-50 [82] are reported. For the latter, it was shown that all losses were fully recoverable losses caused by mass transport, an issue which can be tackled by optimization of the cell design, catalyst layer, and the porous transport layers. In contrast to this, Vincent et al. reported that FAA3-50 already failed within a few hours, whereas supported FAA3-PP-75 could be operated stably for at least 200 h [81]. This shows that the stability strongly depends on the system.

What is missing, is a reliable prediction when membranes will fail. Since this ultimately should take a long time, up to several 10,000 h, and individual membrane samples could fail at quite different times, it is necessary to develop accelerated stress tests, as it was done for PEM Fuel Cells, which have a targeted lifetime of "just" 5000 h in automobile applications. Arico et al. suggested potential cycling between 1 and 1.8 V, to mimic the expected fluctuations when electrolysis is used for grid balancing [82]. This can lead to changes in the water content (if electro-osmotic drag is faster than back diffusion) and in the local temperature. Both will swell and shrink the membranes.

Overall, even though stability is acknowledged to be the bottle neck, not much is known about the already achievable life time in optimized systems.

4 Conclusions

There are research-based membranes and systems, which clearly outperform commercial membranes and their systems. However, they are not easily available and usually still do not fulfill the durability requirement inside of an electrolysis cell. Some membranes seem to be very stable under alkaline conditions—which is a great advancement. The next issues will be to solve the strong swelling and the therefrom resulting softening in hot water, and to investigate the stability against reactive oxygen species.

The main conclusion is that all materials (membrane, ionomer, catalyst, cell design etc.) need to be optimized together. Therefore, it is not possible to exactly rank the commercial membranes based on the available literature data, and any experimental ranking would be limited to a certain system. As a general trend, however, the established membranes FAA3 and A201 have a lower ion conductivity than the newer membrane types Aemion and Sustainion.

Commercial AEMs are usually optimized for only a certain application and operating condition. For example, no data for Sustainion membranes operating in DI Water can be found in the literature, and the technical data sheet of Fumatech FAA-3-50 recommends its use for "electrodialysis for demineralization, desalination applications and others," while FAA-3-PK-75 is also recommended for "alkaline water electrolysis at pH 9–12 and T below 50 °C." Finally, it needs to be remarked that, as far as we are aware, no commercial AEM water electrolysis system uses the discussed commercial membranes, indicating their still relatively low technological readiness level.

However, in contrast to a few years ago, several different AEM chemistries are now commercially available, also in different thicknesses, and as homogenous, reinforced or supported grades. This situation will allow system developers to improve their systems and speed up the research process. The most challenging question is still the life time.

Acknowledgment

This project has received funding from NRF and the Fuel Cells and Hydrogen 2 Joint Undertaking (Grant No. 875118). This Joint Undertaking receives support from the European Union's Horizon 2020 research and innovation programme, Hydrogen Europe and Hydrogen Europe research.

Appendix

Table 3 Commercial membranes and their performance in AEM water electrolyzers[a]

Entry	Company	Detailed membrane type	Ionomer	Anode catalyst	Cathode catalyst	Temperature	Feed	Membrane thickness	Performance at 1.7, 1.8, 1.9 and 2.0 V in A cm^{-2}	Reference
1	Fumatech	FAA-3-50	FAA3-Br	IrO_2	Pt/C	70 °C	1 M KOH	50 μm	0.74 1.15 1.49 1.83	Park et al. [16]
2		FAA-3-50	FAA3-Br	IrO_2	Pt/C	50 °C	1 M KOH	50 μm	0.41 0.73 1.09 1.42	Park et al. [16]
3		FAA3	FAA3	NiCoOx:Fe	Pt/C	50 °C	DI water	130 μm	– 0.11 0.23 0.36	Xu et al. [102]
4		FAA-3-50	–	Nickel foam	Nickel foam	60 °C	10 wt% KOH	55 μm	0.01 0.02 0.02 0.03	Lee et al. [103]
5		FAA-3-50	na	IrO_2	Pt/C	60 °C	1 M KOH	50 μm	0.20 0.32 0.47 0.62	Park et al. [104]
6		FAA-3-50	na	g-CN-CNF-800	Pt/C	60 °C	1 M KOH	50 μm	0.28 0.48 0.72 0.98	Park et al. [104]
7		FAA-3-25	Not disclosed ionomer	Pt/C	Pt/C	60 °C	1 M KOH	25 μm	0.02@2.2V	Fan et al. [105]
8		Fumapem FAA-3-PE-30	Fumion FAA-3-SOLUT-10 solution	Ir black	NiMo/X72	50 °C	1 M KOH	20–30 μm	0.41 0.68 1.00 1.37	Faid et al. [106]
9		Fumapem FAA-3-PE-30	Fumion FAA-3-SOLUT-10 solution	Ir black	Pt/C	50 °C	1 M KOH	20–30 μm	0.63 1.01 1.40 1.80	Faid et al. [106]
10		FAA-3-PK-130	FAA-3-PK-130 solution in DMSO (dimethylsulfoxide) after filtration	$Ce_{0.2}MnFe_{1.8}O_4$	Ni	25 °C	DI water	130 μm	0.11 0.25 – –	Pandiarajan et al. [97]
11		FAA3-50	PTFE	$NiMn_2O_4$/carbon nano fiber	Pt/C	50 °C	DI water	50 μm	– 0.01 0.02 0.04	Busacca et al. [96]
12		FAA3-50	PTFE	$NiMn_2O_4$/carbon nano fiber	Pt/C	60 °C	DI water	50 μm	– 0.02 0.03	Busacca et al. [96]

Table 3 *Continued*

Entry	Company	Detailed membrane type	Ionomer	Anode catalyst	Cathode catalyst	Temperature	Feed	Membrane thickness	Performance at 1.7, 1.8, 1.9 and 2.0 V in A cm^{-2}	Reference
13		FAA3-50	PTFE	$NiMn_2O_4$/carbon nano fiber	Pt/C	50 °C	6 M KOH	50 μm	0.06 0.13 0.18 –	Busacca et al. [96]
14		FAA3-50	PTFE	$NiMn_2O_4$/carbon nano fiber	Pt/C	60 °C	6 M KOH	50 μm	– 0.10 0.14 –	Busacca et al. [96]
15		FAA3-50	FAA3	$NiMn_2O_4$/C	Pt/C	50 °C	1 M KOH	50 μm	– 0.10 0.18 0.27 0.38	Carbone et al. [82]
16		FAA3-40	I_2 (Acta Spa, Italy)	Acta 3030 ($CuCoO_x$)	Acta 4030 (Ni/CeO_2-La_2O_3/C)	60 °C	1% K_2CO_3	40 μm	0.10 0.21 0.37 0.60	Vincent et al. [81]
17		FAA3-PP-75	I_2 (Acta Spa, Italy)	Acta 3030 ($CuCoO_x$)	Acta 4030 (Ni-CeO_2-La_2O_3/C)	60 °C	1% K_2CO_3	80 μm	0.07 0.14 0.24 0.41	Vincent et al. [81]
18		FAA3-PK-75	PTFE	IrO_2	Pt/C	50 °C	0.5 M KOH	75 μm	0.33 0.52 0.70 0.88	Marinkas et al. [69]
19	Tokuyama	A201	AS-4	IrO_2	Pt black	50 °C	DI water	28 μm	0.26 0.40 0.56 0.79	Leng et al. [15]
20		A201	AS-4 (cathode) PTFE (anode)	CuCoOx	Pt/C	50 °C	DI water	28 μm	– 0.01 0.02 0.04	Ito et al. [76]
21		A201	AS-4 (cathode) PTFE (anode)	CuCoOx	Pt/C	50 °C	0.1 wt% K_2CO_3	28 μm	0.07 0.18 0.26 0.40	Ito et al. [76]
22		A201	AS-4 (cathode)	CuCoOx	Pt/C	50 °C	1 wt% K_2CO_3	28 μm	0.12 0.29 0.46 0.68	Ito et al. [76]
23		A201	PTFE (anode)	CuCoOx	Pt/C	50 °C	10 wt% K_2CO_3	28 μm	0.15 0.50 0.97 –	Ito et al. [76]
24		A201	AS-4 (cathode) PTFE (anode)	CuCoOx	Pt/C	50 °C	10 mM of KOH	28 μm	0.11 0.22 0.38	Ito et al. [76]

Table 3 *Continued*

Entry	Company	Detailed membrane type	Ionomer	Anode catalyst	Cathode catalyst	Temperature	Feed	Membrane thickness	Performance at 1.7, 1.8, 1.9 and 2.0 V in A cm^{-2}	Reference
25		A201	No ionomer (PTFE)	$CuCoO_3$	Ni/CeO_2-La_2O_3	43 °C	1 M KOH	28 μm	0.60 0.29 0.52 –	Pavel et al. [83]
26		A-201 with Acta I2 ionomer	No ionomer (PTFE)	$CuCoO_3$	Ni/CeO_2-La_2O_3	43 °C	1% K_2CO_3	28 μm	– 0.19 0.32 0.51	Pavel et al. [83]
27		A-201	I_2 (Acta Spa, Italy)	Acta 3030 ($CuCoO_x$)	Acta 4030 (Ni-CeO_2-La_2O_3/C)	60 °C	1% K_2CO_3	28 μm	– – 0.16 0.37	Vincent et al. [81]
28		A-201	AS-4	CuCoOx	Pt/C	50 °C	10 wt% K_2CO_3	28 μm	0.62 0.18 0.44 0.87	Ito et al. [107]
29		A-201	Nafion	$NiFe_2O_4$	NiFeCo	60 °C	1 M KOH	28 μm	– 0.10 0.26 0.54	Pushkareva et al. [100]
30		A901	No ionomer (10% PTFE)	IrO_2	Pt/C	60 °C	0.1 M KOH	11 μm	0.92 0.36 0.62 0.86	Wu et al. [95]
31		A901	I_2 (Acta Spa, Italy)	Acta 3030 ($CuCoO_x$)	Acta 4030 (Ni/(CeO_2-La_2O_3)/C)	50 °C	1% K_2CO_3	11 μm	1.11 0.10 0.19 0.31	Vincent et al. [108]
32	Ionomr	AF1-HNN8-50-X	FAA-3 Fumion	Ir black	Pt/C	60 °C	1 M KOH	50 μm	0.52 1.03 1.82 –	Fortin et al. [87]
33		AF1-HNN8-50-X	FAA-3 Fumion	Ir black	Pt/C	50 °C	1 M KOH	50 μm	– 0.62 1.00 1.44	Fortin et al. [87]
34		AF1-HNN8-25-X	FAA-3 Fumion	Ir black	Pt/C	50 °C	1 M KOH	25 μm	1.90 0.77 1.27 1.87	Fortin et al. [87]
35		AF1-HNN5-50-X	FAA-3 Fumion	Ir black	Pt/C	50 °C	1 M KOH	50 μm	– 0.43 0.68 0.94	Fortin et al. [87]
36		AF1-HNN5-25-X	FAA-3 Fumion	Ir black	Pt/C	50 °C	1 M KOH	25 μm	1.23 0.61 0.96 1.35	Fortin et al. [87]

Table 3 *Continued*

Entry	Company	Detailed membrane type	Ionomer	Anode catalyst	Cathode catalyst	Temperature	Feed	Membrane thickness	Performance at 1.7, 1.8, 1.9 and 2.0 V in A cm^{-2}	Reference
37		AEMION	Nafion	$NiFe_2O_4$	NiFeCo	60 °C	1 M KOH	38 μm	1.77 0.04 0.13 0.31 0.63	Pushkareva et al. [100]
38		AEMION	Nafion	$NiFe_2O_4$	NiFeCo	60 °C	0.1 M KOH	38 μm	0.01 0.03 0.07 0.13	Pushkareva et al. [100]
39	Dioxide materials	Sustainion	Nafion	$NiFe_2O_4$	NiFeCo	60 °C	1 M KOH	50 μm	0.05 0.16 0.43 0.94	Pushkareva et al. [100]
40		Sustainion 37-50		NiFe	NiFeCo	60 °C	1 M KOH	50 μm	0.16 0.47 1.01 1.75	Liu et al. [17] and Kaczuret al. [91]
41		Sustainion 37–50		IrO_2	Pt	60 °C	1 M KOH	50 μm	1.99 3.33 –	Kaczuret al. [91]
42		Sustainion X37-50 grade T	Sustanion XB-7	IrO_2	Pt/HSC (47% Pt	60 °C	0.1 M KHCO3	50 μm	0.72[b] – –	Anderson et al. [109]
43	Orion polymer	TPN1-100 (same materials TM1)	Tokuyama AS-4	PGM	PGM	50 °C	1 M NaOH	Not reported—TM1 may be thinner, allowing higher performance	– – – 0.05	Park et al. [94]

[a]Data were extracted from literature with DigitizeIt (www.digitizeIT.de).
[b]Extrapolated value.

References

[1] Caglayan, D. G., Weber, N., Heinrichs, H. U., Linßen, J., Robinius, M., Kukla, P. A., and Stolten, D., 2020, "Technical Potential of Salt Caverns for Hydrogen Storage in Europe," Int. J. Hydr. Energy, **45**(11), pp. 6793–6805.

[2] Schalenbach, M., Lueke, W., and Stolten, D., 2016, "Hydrogen Diffusivity and Electrolyte Permeability of the Zirfon PERL Separator for Alkaline Water Electrolysis," J. Electrochem. Soc., **163**(14), pp. F1480–F1488.

[3] Carmo, M., Fritz, D. L., Mergel, J., and Stolten, D., 2013, "A Comprehensive Review on PEM Water Electrolysis," Int. J. Hydr. Energy, **38**(12), pp. 4901–4934.

[4] Schalenbach, M., Zeradjanin, A. R., Kasian, O., Cherevko, S., and Mayrhofer, K. J., 2018, "A Perspective on Low-Temperature Water Electrolysis-Challenges in Alkaline and Acidic Technology," Int. J. Electrochem. Sci., **13**(2), pp. 1173–1226.

[5] Ayers, K. E., Capuano, C., and Anderson, E. B., 2012, "Recent Advances in Cell Cost and Efficiency for PEM-Based Water Electrolysis," ECS Trans., **41**(10), pp. 15–22.

[6] Ayers, K. E., Moulthrop, L., and Anderson, E. B., 2012, "Hydrogen Infrastructure Challenges and Solutions," ECS Trans., **41**(46), pp. 75–83.

[7] Barbir, F., 2005, "PEM Electrolysis for Production of Hydrogen From Renewable Energy Sources," Sol. Energy, **78**(5), pp. 661–669.

[8] Ayers, K. E., Anderson, E. B., Capuano, C., Carter, B., Dalton, L., Hanlon, G., Manco, J., and Niedzwiecki, M., 2010, "Research Advances Towards Low Cost, High Efficiency PEM Electrolysis," ECS Trans., **33**(1), pp. 3–15.

[9] 1510 USD per troy oz, http://www.metalary.com/iridium-price/, Accessed March 10, 2020

[10] Geinitz, C., 2020, "Wasserstoff wird ausgebremst," Frankurter Allgemeine Zeitung, https://www.faz.net/aktuell/wirtschaft/digitec/wasserstofftechnik-wasserstoff-als-gruener-konjunktur-motor-16787360.html, Accessed May 29, 2020.

[11] Vincent, I., and Bessarabov, D., 2018, "Low Cost Hydrogen Production by Anion Exchange Membrane Electrolysis: A Review," Renew. Sustain. Energy Rev., **81**, pp. 1690–1704.

[12] Cho, M. K., Lim, A., Lee, S. Y., Kim, H. J., Yoo, S. J., Sung, Y. E., Park, H. S., and Jang, J. H., 2017, "A Review on Membranes and Catalysts for Anion Exchange Membrane Water Electrolysis Single Cells," J. Electrochem. Sci. Technol., **8**, pp. 183–196.

[13] Miller, H. A., Bouzek, K., Hnat, J., Loos, S., Bernäcker, C. I., Weißgäerber, T., Röntsch, L., and Meier-Haack, J., 2020, "Green Hydrogen From Anion Exchange Membrane Water Electrolysis: A Review of Recent Developments in Critical Materials and Operating Conditions," Sust. Energy Fuels, **4**(5), pp. 2114–2133.

[14] Wu, X., and Scott, K., 2011, "$CuxCo_{3-x}O_4$ ($0 \leq x < 1$) Nanoparticles for Oxygen Evolution in High Performance Alkaline Exchange Membrane Water Electrolysers," J. Mater. Chem. A, **21**, pp. 12344–12351.

[15] Leng, Y., Chen, G., Mendoza, A. J., Tighe, T. B., Hickner, M. A., and Wang, C. Y., 2012, "Solid-State Water Electrolysis With an Alkaline Membrane," J. Am. Chem. Soc., **134**(22), pp. 9054–9057.

[16] Park, J. E., Kang, S. Y., Oh, S. H., Kim, J. K., Lim, M. S., Ahn, C. Y., Cho, Y. H., and Sung, Y. E., 2019, "High-Performance Anion-Exchange Membrane Water Electrolysis," Electrochim. Acta, **295**, pp. 99–106.

[17] Liu, Z., Sajjad, S. D., Gao, Y., Yang, H., Kaczur, J. J., and Masel, R. I., 2017, "The Effect of Membrane on an Alkaline Water Electrolyzer," Int. J. Hydr. Energy, **42**(50), pp. 29661–29665.

[18] Münchinger, A., and Kreuer, K. D., 2019, "Selective Ion Transport Through Hydrated Cation and Anion Exchange Membranes I. The Effect of Specific Interactions," J. Membr. Sci., **592**, p. 117372.

[19] Li, D., Park, E. J., Zhu, W., Shi, Q., Zhou, Y., Tian, H., Lin, Y., Serov, A., Zulevi, B., Baca, E. D., Fujimoto, C., Chung, H. T., and Kim, Y. S., 2020, "Highly Quaternized Polystyrene Ionomers for High Performance Anion Exchange Membrane Water Electrolysers," Nat. Energy, **5**, pp. 378–385.

[20] Li, D., Matanovic, I., Lee, A. S., Park, E. J., Fujimoto, C., Chung, H. T., and Kim, Y. S., 2019, "Phenyl Oxidation Impacts the Durability of Alkaline Membrane Water Electrolyzer," ACS Appl. Mater. Interf., **11**, pp. 9696–9701.

[21] Varcoe, J. R., Atanassov, P., Dekel, D. R., Herring, A. M., Hickner, M. A., Kohl, P. A., Kucernak, A. R., Mustain, W. E., Nijmeijer, K., Scott, K., and Xu, T., 2014, "Anion-Exchange Membranes in Electrochemical Energy Systems," Energy Environ. Sci., **7**(10), pp. 3135–3191.

[22] Merle, G., Wessling, M., and Nijmeijer, K., 2011, "Anion Exchange Membranes for Alkaline Fuel Cells: A Review," J. Membr. Sci., **377**(1–2), pp. 1–35.

[23] Arges, C. G., and Zhang, L., 2018, "Anion Exchange Membranes' Evolution Toward High Hydroxide Ion Conductivity and Alkaline Resiliency," ACS Appl. Energy Mater., **1**(7), pp. 2991–3012.

[24] Arges, C. G., and Ramani, V., 2013, "Two-Dimensional NMR Spectroscopy Reveals Cation-Triggered Backbone Degradation in Polysulfone-Based Anion Exchange Membranes," Proc. Nat. Ac. Sci., **110**(7), pp. 2490–2495.

[25] Fujimoto, C., Kim, D. S., Hibbs, M., Wrobleski, D., and Kim, Y. S., 2012, "Backbone Stability of Quaternized Polyaromatics for Alkaline Membrane Fuel Cells," J. Membr. Sci., **423**, pp. 438–449.

[26] Park, E. J., and Kim, Y. S., 2018, "Quaternized Aryl Ether-Free Polyaromatics for Alkaline Membrane Fuel Cells: Synthesis, Properties, and Performance—A Topical Review," J. Mater. Chem. A, **6**(32), pp. 15456–15477.

[27] Chempath, S., Boncella, J. M., Pratt, L. R., Henson, N., and Pivovar, B. S., 2010, "Density Functional Theory Study of Degradation of Tetraalkylammonium Hydroxides," J. Phys. Chem. C, **114**(27), pp. 11977–11983.

[28] Müller, J., Zhegur, A., Krewer, U., Varcoe, J. R., and Dekel, D. R., 2020, "Practical Ex-Situ Technique To Measure the Chemical Stability of Anion-Exchange Membranes Under Conditions Simulating the Fuel Cell Environment," ACS Mater. Lett., **2**, pp. 168–173.

[29] Kim, D. S., Fujimoto, C. H., Hibbs, M. R., Labouriau, A., Choe, Y. K., and Kim, Y. S., 2013, "Resonance Stabilized Perfluorinated Ionomers for Alkaline Membrane Fuel Cells," Macromolecules, **46**(19), pp. 7826–7833.

[30] Hugar, K. M., KostalikH. A., and IV Coates, G. W., 2015, "Imidazolium Cations With Exceptional Alkaline Stability: A Systematic Study of Structure–Stability Relationships," J. Am. Chem. Soc., **137**(27), pp. 8730–8737.

[31] Kutz, R. B., Chen, Q., Yang, H., Sajjad, S. D., Liu, Z., and Masel, I. R., 2017, "Sustainion Imidazolium-Functionalized Polymers for Carbon Dioxide Electrolysis," Energy Technol., **5**(6), pp. 929–936.

[32] Gu, S., Cai, R., Luo, T., Chen, Z., Sun, M., Liu, Y., He, G., and Yan, Y., 2009, "A Soluble and Highly Conductive Ionomer for High-Performance Hydroxide Exchange Membrane Fuel Cells," Angew. Chem. Int. Ed., **48**(35), pp. 6499–6502.

[33] Gu, S., Wang, J., Kaspar, R. B., Fang, Q., Zhang, B., Coughlin, E. B., and Yan, Y., 2015, "Permethyl Cobaltocenium (Cp* 2 Co+) as an Ultra-Stable Cation for Polymer Hydroxide-Exchange Membranes," Sci. Rep., **5**, p. 11668.

[34] Marino, M. G., and Kreuer, K. D., 2015, "Alkaline Stability of Quaternary Ammonium Cations for Alkaline Fuel Cell Membranes and Ionic Liquids," ChemSusChem, **8**(3), pp. 513–523.

[35] Pearman, B. P., Mohajeri, N., Brooker, R. P., Rodgers, M. P., Slattery, D. K., Hampton, M. D., Cullen, D. A., and Seal, S., 2013, "The Degradation Mitigation Effect of Cerium Oxide in Polymer Electrolyte Membranes in Extended Fuel Cell Durability Tests," J. Power Sour., **225**, pp. 75–83.

[36] Zhao, N., Xie, Z., and Shi, Z., 2019, "Understanding of Nafion Membrane Additive Behaviors in Proton Exchange Membrane Fuel Cell Conditioning," J. Electrochem. Energy Conv. Stor., **16**(1), p. 011011.

[37] Russo, V., Protasova, L., Turco, R., De Croon, M. H. J. M., Hessel, V., and Santacesaria, E., 2013, "Hydrogen Peroxide Decomposition on Manganese Oxide Supported Catalyst: From Batch Reactor to Continuous Microreactor," Ind. Eng. Chem. Res., **52**(23), pp. 7668–7676.

[38] Špalek, O., Balej, J., and Paseka, I., 1982, "Kinetics of the Decomposition of Hydrogen Peroxide in Alkaline Solutions," J. Chem. Soc., Faraday Trans. 1: Phys. Chem. Condensed Phases., **78**(8), pp. 2349–2359.

[39] Zhang, Y., Parrondo, J., Sankarasubramanian, S., and Ramani, V., 2017, "Detection of Reactive Oxygen Species in Anion Exchange Membrane Fuel Cells Using In situ Fluorescence Spectroscopy," ChemSusChem, **10**(15), pp. 3056–3062.

[40] Parrondo, J., Wang, Z., Jung, M. S. J., and Ramani, V., 2016, "Reactive Oxygen Species Accelerate Degradation of Anion Exchange Membranes Based on Polyphenylene Oxide in Alkaline Environments," Phys. Chem. Chem. Phys., **18**(29), pp. 19705–19712.

[41] Si, K., Dong, D., Wycisk, R., and Litt, M., 2012, "Synthesis and Characterization of Poly (Para-Phenylene Disulfonic Acid), Its Copolymers and Their n-Alkylbenzene Grafts as Proton Exchange Membranes: High Conductivity at Low Relative Humidity," J. Mater. Chem., **22**(39), pp. 20907–20917.

[42] Noh, S., Jeon, J. Y., Adhikari, S., Kim, Y. S., and Bae, C., 2019, "Molecular Engineering of Hydroxide Conducting Polymers for Anion Exchange Membranes in Electrochemical Energy Conversion Technology," Acc. Chem. Res., **52**, pp. 2745–2755.

[43] Gubler, L., and Scherer, G. G., 2009, "Radiation-Grafted Proton Conducting Membranes," *Handbook of Fuel Cells: Advances in Electrocatalysis, Materials, Diagnostics and Durability*, Vol. 5, W Vielstich, HA Gasteiger, and H Yokokawa, eds, John Wiley & Sons, Chichester, Chap. 20, pp. 313–321.

[44] Jeon, J. Y., Tian, D., Pagels, M. K., and Bae, C., 2019, "Efficient Preparation of Styrene Block Copolymer Anion Exchange Membranes via One-Step Friedel–Crafts Bromoalkylation With Alkenes," Org. Proc. Res. Dev., **23**(8), pp. 1580–1586.

[45] Žitka, J., Peter, J., Galajdová, B., Pavlovec, L., Pientka, Z., Paidar, M., Hnát, J., and Bouzek, K., 2019, "Anion Exchange Membranes and Binders Based on Polystyrene-Block-Poly (Ethylene-ran-Butylene)-Block-Polystyrene Copolymer for Alkaline Water Electrolysis," Desal. Water Treatm., **142**, pp. 90–97.

[46] Poynton, S. D., Slade, R. C., Omasta, T. J., Mustain, W. E., Escudero-Cid, R., Ocón, P., and Varcoe, J. R., 2014, "Preparation of Radiation-Grafted Powders for use as Anion Exchange Ionomers in Alkaline Polymer Electrolyte Fuel Cells," J. Mater. Chem. A, **2**(14), pp. 5124–5130.

[47] Wang, L., Peng, X., Mustain, W. E., and Varcoe, J. R., 2019, "Radiation-Grafted Anion-Exchange Membranes: The Switch From Low-to High-Density Polyethylene Leads to Remarkably Enhanced Fuel Cell Performance," Energy Environ. Sci., **12**(5), pp. 1575–1579.

[48] Lee, W. H., Park, E. J., Han, J., Shin, D. W., Kim, Y. S., and Bae, C., 2017, "Poly (Terphenylene) Anion Exchange Membranes: the Effect of Backbone Structure on Morphology and Membrane Property," ACS Macro Lett., **6**(5), pp. 566–570.

[49] Ren, R., Zhang, S., Miller, H. A., Vizza, F., Varcoe, J. R., and He, Q., 2019, "Facile Preparation of an Ether-Free Anion Exchange Membrane With Pendant Cyclic Quaternary Ammonium Groups," ACS Appl. Energy Mater., **2**(7), pp. 4576–4581.

[50] Henkensmeier, D., Kim, H. J., Lee, H. J., Lee, D. H., Oh, I. H., Hong, S. A., Nam, S. W., and Lim, T. H., 2011, "Polybenzimidazolium-Based Solid Electrolytes," Macromol. Mater. Eng., **296**(10), pp. 899–908.

[51] Thomas, O. D., Soo, K. J., Peckham, T. J., Kulkarni, M. P., and Holdcroft, S., 2011, "Anion Conducting Poly (Dialkyl Benzimidazolium) Salt," Polym. Chem., **2**(8), pp. 1641–1643.

[52] Thomas, O. D., Soo, K. J., Peckham, T. J., Kulkarni, M. P., and Holdcroft, S., 2012, "A Stable Hydroxide-Conducting Polymer," J. Am. Chem. Soc., **134**(26), pp. 10753–10756.
[53] Henkensmeier, D., Cho, H. R., Kim, H. J., Kirchner, C. N., Leppin, J., Dyck, A., Jang, J. H., Cho, E., Nam, S. W., and Lim, T. H., 2012, "Polybenzimidazolium Hydroxides–Structure, Stability and Degradation," Polym. Degrad. Stability, **97**(3), pp. 264–272.
[54] Henkensmeier, D., Kim, H. J., Jang, J. H., Cho, E., Kim, S. K., Oh, I. H., Hong, S. A., Nam, S. W., and Lim, T. H., 2018, "Polybenzimidazolium Based Solid Electrolytes," Korean Patent KR 1020110033416, filed 2011.04.11.
[55] Lee, Y., Kim, S., Maljusch, A., Conradi, O., Kim, H. J., Jang, J. H., Han, J., Kim, J., and Henkensmeier, D., 2019, "Polybenzimidazole Membranes Functionalised With 1-Methyl-2-Mesitylbenzimidazolium Ions via a Hexyl Linker for Use in Vanadium Flow Batteries," Polymer, **174**, pp. 210–217.
[56] Wang, X., Chen, W., Yan, X., Li, T., Wu, X., Zhang, Y., Zhang, F., Pang, B., and He, G., 2020, "Pre-Removal of Polybenzimidazole Anion to Improve Flexibility of Grafted Quaternized Side Chains for High Performance Anion Exchange Membranes," J. Power Sour., **451**, p. 227813.
[57] Krishnan, N. N., Henkensmeier, D., Jang, J. H., and Kim, H. J., 2014, "Nanocomposite Membranes for Polymer Electrolyte Fuel Cells," Macromol. Mater. Eng., **299**(9), pp. 1031–1041.
[58] https://ec.europa.eu/info/funding-tenders/opportunities/portal/screen/opportunities/topic-details/fch-02-4-2019;freeTextSearchKeyword=AEM;typeCodes=1;statusCodes=31094501,31094502;programCode=H2020;programDivisionCode=null;focusAreaCode=null;crossCuttingPriorityCode=null;callCode=Default;sortQuery=openingDate;orderBy=asc;onlyTenders=false, Accessed March 12, 2020.
[59] Krishnan, N. N., Henkensmeier, D., Jang, J. H., Hink, S., Kim, H. J., Nam, S. W., and Lim, T. H., 2014, "Locally Confined Membrane Modification of Sulfonated Membranes for Fuel Cell Application," J. Membr. Sci., **454**, pp. 174–183.
[60] DuPont Nafion Bulletin E-63118-1, 2000, Nafion Perfluorinated Membranes User's Guide.
[61] Henkensmeier, D., and Gubler, L., 2014, "Shape Memory Effect in Radiation Grafted ion Exchange Membranes," J. Mat. Chem. A, **2**(25), pp. 9482–9485.
[62] Hink, S., Henkensmeier, D., Jang, J. H., Kim, H. J., Han, J., and Nam, S. W., 2015, "Reduced In-Plane Swelling of Nafion by a Biaxial Modification Process," Macromol. Chem. Phys., **216**(11), pp. 1235–1243.
[63] Kressman, T. R. E., 1950, "Ion Exchange Resin Membranes and Resin-Impregnated Filter Paper," Nature, **165**(4197), pp. 568–568.
[64] Perry, J. Jr., 1960, "Anion-Exchange Membrane Fuel Cells," Proc. Ann. Power Sources Conf., **14**, pp. 50–52.
[65] Ledjeff, K., Ahn, J., and Heinzel, A., 1990, "Vergleich von Elektrolyseur und Brennstoffzelle mit Polymerem Festelektrolyt." *DECHEMA-Monographie* (Vol. 121). VCH, Weinheim, p. 109.
[66] Kraglund, M. R., Carmo, M., Schiller, G., Ansar, S. A., Aili, D., Christensen, E., and Jensen, J. O., 2019, "Ion-Solvating Membranes as a New Approach Towards High Rate Alkaline Electrolyzers," Energy Environ. Sci., **12**(11), pp. 3313–3318.
[67] Schuster, M., 2014, *(Fumatech), at EMEA Workshop*, Bad Zwischenahn, Germany.
[68] Isomura, T., 2016, *(Tokuyama), at EMEA Workshop*, Bad Zwischenahn, Germany.
[69] Marinkas, A., Struźyńska-Piron, I., Lee, Y., Lim, A., Park, H. S., Jang, J. H., Kim, H. J., Kim, J., Maljusch, A., Conradi, O., and Henkensmeier, D., 2018, "Anion-Conductive Membranes Based on 2-Mesityl-Benzimidazolium Functionalised Poly (2, 6-Dimethyl-1, 4-Phenylene Oxide) and Their Use in Alkaline Water Electrolysis," Polymer, **145**, pp. 242–251.
[70] Ziv, N., Mustain, W. E., and Dekel, D. R., 2018, "The Effect of Ambient Carbon Dioxide on Anion-Exchange Membrane Fuel Cells," ChemSusChem, **11**(7), pp. 1136–1150.
[71] Ziv, N., and Dekel, D. R., 2018, "A Practical Method for Measuring the True Hydroxide Conductivity of Anion Exchange Membranes," Electrochem. Commun., **88**, pp. 109–113.
[72] Cao, X., Novitski, D., and Holcroft, S., 2019, "Visualization of Hydroxide Ion Formation Upon Electrolytic Water Splitting in an Anion Exchange Membrane," ACS Mater. Lett., **1**, pp. 362–366.
[73] Höfner, T., 2016, "Development of Membrane Electrode Assemblies for the Anion Exchange Membrane Water Electrolysis," PhD thesis, RWTH, Aachen, http://publications.rwth-aachen.de/record/661803/files/661803.pdf
[74] Novitski, D., Kosakian, A., Weissbach, T., Secanell, M., and Holdcroft, S., 2016, "Electrochemical Reduction of Dissolved Oxygen in Alkaline, Solid Polymer Electrolyte Films," J. Am. Chem. Soc., **138**, pp. 15465–15472.
[75] Gunasekara, I., Lee, M., Abbott, D., and Mukerjee, S., 2012, "Mass Transport and Oxygen Reduction Kinetics at an Anion Exchange Membrane Interface: Microelectrode Studies on Effect of Carbonate Exchange," ECS Electrochem. Lett., **1**, pp. F16–F19.
[76] Ito, H., Kawaguchi, N., Someya, S., Munakata, T., Miyazaki, N., Ishida, M., and Nakano, A., 2018, "Experimental Investigation of Electrolytic Solution for Anion Exchange Membrane Water Electrolysis," Int. J. Hydrogen Energy, **43**(36), pp. 17030–17039.
[77] Cho, M. K., Park, H. Y., Lee, J. J., Kim, H.-J., Lim, A., Henkensmeier, D., Yoo, S. J., Kim, J. Y., Lee, S. Y., Park, H. S., and Jang, J. H., 2018, "Alkaline Anion Exchange Membrane Water Electrolysis: Effects of Electrolyte Feed Method and Electrode Binder Content," J. Power Sources, **382**, pp. 22–29.
[78] Konovalova, A., Kim, H., Kim, S., Lim, A., Park, H. S., Kraglund, M. R., Aili, D., Jang, J. H., Kim, H. J., and Henkensmeier, D., 2018, "Blend Membranes of Polybenzimidazole and an Anion Exchange Ionomer (FAA3) for Alkaline Water Electrolysis: Improved Alkaline Stability and Conductivity," J. Membr. Sci., **564**, pp. 653–662.
[79] Luo, X., Wright, A., Weissbach, T., and Holdcroft, S., 2018, "Water Permeation Through Anion Exchange Membranes," J. Power Sources, **375**, pp. 442–451.
[80] Lim, A., Kim, H. J., Henkensmeier, D., Yoo, S. J., Kim, J. Y., Lee, S. Y., Sung, Y. E., Jang, J. H., and Park, H. S., 2019, "A Study on Electrode Fabrication and Operation Variables Affecting the Performance of Anion Exchange Membrane Water Electrolysis," J. Ind. Eng. Chem., **76**, pp. 410–418.
[81] Vincent, I., Kruger, A., and Bessarabov, D., 2017, "Development of Efficient Membrane Electrode Assembly for Low Cost Hydrogen Production by Anion Exchange Membrane Electrolysis," Int. J. Hydr. Energy, **42**(16), pp. 10752–10761.
[82] Carbone, A., Zignani, S. C., Gatto, I., Trocino, S., and Aricò, A. S., 2020, "Assessment of the FAA3-50 Polymer Electrolyte in Combination With a NiMn2O4 Anode Catalyst for Anion Exchange Membrane Water Electrolysis," Int. J. Hydr. Energy, **45**(16), pp. 9285–9292.
[83] Pavel, C. C., Cecconi, F., Emiliani, C., Santiccioli, S., Scaffidi, A., Catanorchi, S., and Comotti, M., 2014, "Highly Efficient Platinum Group Metal Free Based Membrane-Electrode Assembly for Anion Exchange Membrane Water Electrolysis," Angew. Chem. Int. Ed., **53**(5), pp. 1378–1381.
[84] Wright, A. G., and Holdcroft, S., 2014, "Hydroxide-Stable Ionenes," ACS Macro Lett., **3**(5), pp. 444–447.
[85] Wright, A. G., Fan, J., Britton, B., Weissbach, T., Lee, H.-F., Kitching, E. A., Peckham, T. J., and Holdcroft, S., 2016, "Hexamethyl-p-terphenyl Poly(Benzimidazolium): A Universal Hydroxide-Conducting Polymer for Energy Conversion Devices," Energy Envir. Sci., **9**, pp. 2130–2142.
[86] Wang, L., Weissbach, T., Reissner, R., Ansar, A., Gago, A. S., Holdcroft, S., and Friedrich, K. A., 2019, "High Performance Anion Exchange Membrane Electrolysis Using Plasma-Sprayed, Non-Precious-Metal Electrodes," ACS Appl. Energy Mater., **2**(11), pp. 7903–7912.
[87] Fortin, P., Khoza, T., Cao, X., Martinsen, S. Y., Barnett, A. O., and Holdcroft, S., 2020, "High-Performance Alkaline Water Electrolysis Using Aemion™ Anion Exchange Membranes," J. Power Sour., **451**, p. 227814.
[88] Buttler, A., and Spliethoff, H., 2018, "Current Status of Water Electrolysis for Energy Storage, Grid Balancing and Sector Coupling via Power-to-Gas and Power-to-Liquids: A Review," Renew. Sustain. Energy Rev., **82**, pp. 2440–2454.
[89] Weber, R. L., Ye, Y., Banik, S. M., Elabd, Y. A., Hickner, M. A., and Mahanthappa, M. K., 2011, "Thermal and Ion Transport Properties of Hydrophilic and Hydrophobic Polymerized Styrenic Imidazolium Ionic Liquids," J. Polym. Sci.: Part B: Polym. Phys., **49**, pp. 1287–1296.
[90] Masel, R., 2017, *Polymers for Fuel Cells, Energy Storage, and Conversion*, Pacific Grove, CA.
[91] Kaczur, J. J., Yang, H., Liu, Z., Sajjad, S. D., and Masel, R. I., 2018, "Carbon Dioxide and Water Electrolysis Using New Alkaline Stable Anion Membranes," Front. Chem., **6**, p. 263.
[92] Jannasch, P., and Weiber, E. A., 2016, "Configuring Anion-Exchange Membranes for High Conductivity and Alkaline Stability by Using Cationic Polymers With Tailored Side Chains," Macromol. Chem. Phys., **217**(10), pp. 1108–1118.
[93] Meek, K. M., Antunes, C. M., Strasser, D., Owczarczyk, Z. R., Neyerlin, A., and Pivovar, B. S., 2019, "High-Throughput Anion Exchange Membrane Characterization at NREL," ECS Trans., **92**(8), pp. 723–731.
[94] Park, E. J., Capuano, C. B., Ayers, K. E., and Bae, C., 2018, "Chemically Durable Polymer Electrolytes for Solid-State Alkaline Water Electrolysis," J. Power Sour., **375**, pp. 367–372.
[95] Wu, T., Sun, S., Song, J., Xi, S., Du, Y., Chen, B., Sasangka, W. A., Liao, H., Gan, C. L., Scherer, G. G., and Zeng, L., 2019, "Iron-Facilitated Dynamic Active-Site Generation on Spinel $CoAl_2O_4$ With Self-Termination of Surface Reconstruction for Water Oxidation," Nature Cat., **2**(9), pp. 763–772.
[96] Busacca, C., Zignani, S. C., Di Blasi, A., Di Blasi, O., Faro, M. L., Antonucci, V., and Aricò, A. S., 2019, "Electrospun $NiMn_2O_4$ and $NiCo_2O_4$ Spinel Oxides Supported on Carbon Nanofibers as Electrocatalysts for the Oxygen Evolution Reaction in an Anion Exchange Membrane-Based Electrolysis Cell," Int. J. Hydr. Energy, **44**(38), pp. 20987–20996.
[97] Pandiarajan, T., Berchmans, L. J., and Ravichandran, S., 2015, "Fabrication of Spinel Ferrite Based Alkaline Anion Exchange Membrane Water Electrolysers for Hydrogen Production," RSC Adv., **5**(43), pp. 34100–34108.
[98] King, L. A., Hubert, M. A., Capuano, C., Manco, J., Danilovic, N., Valle, E., Hellstern, T. R., Ayers, K., and Jaramillo, T. F., 2019, "A Non-Precious Metal Hydrogen Catalyst in a Commercial Polymer Electrolyte Membrane Electrolyser," Nat. Nanotechnol., **14**(11), pp. 1071–1074.
[99] Kamcev, J., Paul, D. R., and Freeman, B. D., 2015, "Ion Activity Coefficients in Ion Exchange Polymers: Applicability of Manning's Counterion Condensation Theory," Macromol., **48**(21), pp. 8011–8024.
[100] Pushkareva, I. V., Pushkarev, A. S., Grigoriev, S. A., Modisha, P., and Bessarabov, D. G., 2019, "Comparative Study of Anion Exchange Membranes for Low-Cost Water Electrolysis," Int. J. Hydr. Energy.
[101] Bender, G., Carmo, M., Smolinka, T., Gago, A., Danilovic, N., Mueller, M., Ganci, F., Fallisch, A., Lettenmeier, P., Friedrich, K. A., Ayers, K., Pivovar, B., Mergel, J., and Stolten, D., 2019, "Initial Approaches in Benchmarking and Round Robin Testing for Proton Exchange Membrane Water Electrolyzers," Int. J. Hydrogen Energy, **44**(18), pp. 9174–9187.
[102] Xu, D., Stevens, M. B., Cosby, M. R., Oener, S. Z., Smith, A. M., Enman, L. J., Ayers, K. E., Capuano, C. B., Renner, J. N., Danilovic, N., and Li, Y., 2018, "Earth-Abundant Oxygen Electrocatalysts for Alkaline

Anion-Exchange-Membrane Water Electrolysis: Effects of Catalyst Conductivity and Comparison With Performance in Three-Electrode Cells," ACS Catal., **9**(1), pp. 7–15.
[103] Lee, N., Duong, D. T., and Kim, D., 2018, "Cyclic Ammonium Grafted Poly (Arylene Ether Ketone) Hydroxide Ion Exchange Membranes for Alkaline Water Electrolysis With High Chemical Stability and Cell Efficiency," Electrochim. Acta, **271**, pp. 150–157.
[104] Park, J. E., Kim, M.-J., Lim, M. S., Kang, S. Y., Kim, J. K., Oh, S.-H., Her, M., Cho, Y.-H., and Sung, Y.-E., 2018, "Graphitic Carbon Nitride-Carbon Nanofiber as Oxygen Catalyst in Anion-Exchange Membrane Water Electrolyzer and Rechargeable Metal–Air Cells," Appl. Catal., B, **237**, pp. 140–148.
[105] Fan, J., Willdorf-Cohen, S., Schibli, E. M., Paula, Z., Li, W., Skalski, T. J., Sergeenko, A. T., Hohenadel, A., Frisken, B. J., Magliocca, E., and Mustain, W. E., 2019, "Poly (bis-Arylimidazoliums) Possessing High Hydroxide ion Exchange Capacity and High Alkaline Stability," Nat. Commun., **10**(1), pp. 1–10.
[106] Faid, A. Y., Oyarce Barnett, A., Seland, F., and Sunde, S., 2018, "Highly Active Nickel-Based Catalyst for Hydrogen Evolution in Anion Exchange Membrane Electrolysis," Catalysts., **8**(12), p. 614.
[107] Ito, H., Kawaguchi, N., Someya, S., and Munakata, T., 2019, "Pressurized Operation of Anion Exchange Membrane Water Electrolysis," Electrochim. Acta, **297**, pp. 188–196.
[108] Vincent, I., Kruger, A., and Bessarabov, D., 2018, "Hydrogen Production by Water Electrolysis With an Ultrathin Anion-Exchange Membrane (AEM)," I. J. Electrochem. Sci., **13**, pp. 11347–11358.
[109] Anderson, G. C., Pivovar, B. S., and Alia, S. M., 2020, "Establishing Performance Baselines for the Oxygen Evolution Reaction in Alkaline Electrolytes," J. Electrochem. Soc., **167**(4), p. 044503.